RESEARCH PAPER

Synthesis of API intermediate by using mixed metal oxide nanocatalyst

Devidas B Patil[a, b], Sharda Gadale, Sathiyanarayanan Lohidasan[b], Aarif Shaikh[b], Suhas Mohite[a*]

[a*]Department of Chemistry, Bharati Vidyapeeth (Deemed to be university), Yashwantrao Mohite College, Pune-411038, Maharashtra, India.

Email: suhas.mohite@bharatividyapeeth.edu

[b]Poona College of Pharmacy Bharati Vidyapeeth (Deemed to be university), Pune 411038, Maharashtra, India.

ABSTRACT

Introduction:- The development of new heterogeneous catalysts for the nitration of aromatic reaction using green chemistry is the need of hour across the globe. The present study shows simple and efficient aromatic nitration protocol with novel nanocatalyst Cu/Mo/SiO_2. These novel catalysts are more environmentally friendly and non-hazardous for handling.

Methods – The present study indicates synthesis of novel nanocatalyst Cu/Mo/SiO_2 using sol–gel method. The newly generated nano catalyst has been utilized for the efficient aromatic nitration reaction to afford regioselective products.

Results- The novel nanocatalyst Cu/Mo/SiO_2 was prepared successfully and implemented for the nitration reaction. Several substituted aromatic compounds were converted to the corresponding nitrated regio-isomers using mild condition.

Discussion:- The newly generated nanocatalyst Cu/Mo/SiO_2 has been well characterized by XRD, SEM, TEM, IR, and EDX analyses. All synthesized products were analysed by ^{1}H NMR, ^{13}C NMR, and melting points.

Conclusion - This is the efficient, mild and green approach for the synthesis of nitrated compounds using novel heterogenous catalyst Cu/Mo/SiO_2. This protocol is more safe, environmentally friendly and sustainable for several compounds.

Keywords: Novel nanocatalysts; SolGel Technique; Aromatic Nitration; Green Chemistry; Cu/Mo/SiO_2 Catalyst.

How to cite this article: Devidas B Patil, Sharda Gadale, Sathiyanarayanan Lohidasan, Aarif Shaikh, Suhas Mohite, Synthesis Of API Intermediate by Using Nano Mixed Metal Oxide Catalyst, Int J Drug Deliv Technol. 2026;16(87s): 1807-1827; DOI: 10.25258/ijddt.16.87s.194

1. Introduction

The development of safe, efficient, robust, chemically benign processes for the synthesis of active pharmaceutical ingredients (APIs) intermediates is critical and challenging in the pharmaceutical and chemical industries [1-4]. The application of green chemistry is essential worldwide to make processes simpler, more efficient and environmentally friendly while reducing chemical waste [5-9]. Synthesis of new organic compounds via green approach is more beneficial to have high atom economy. Green synthesis is an emerging tool for the invention of the chemical and pharmaceutical industries for developing new compounds for sustainable product development [10-13].

In recent years, nanostructured catalysts have been attracted growing attention towards high surface area, chemical stability, and eco-friendly profiles[14-18]. The hetrogenious catalyst Cu/Mo/SiO_2 are particularly attractive due to their non-toxicity, high thermal stability (up to 900 °C), and corrosion resistance[19-22]. Surface methodologies of Cu-Mo-Si were investigated and identified by macroscopic methods[23-25]. Mix-metal oxide have been widely explored in heterogeneous catalysis. Heterogeneous catalyst plays pivotal role for the chemicals synthesis, energy transformation and the biological degradation[26-27].

Aromatic nitration is a key and very useful reaction for the synthesis of dyes, agrochemicals, and pharmaceutical intermediates[28-30]. Traditional nitration processes commonly involve the use of mixed acid systems (fuming HNO_3 and H_2SO_4), which are highly hazardous, generate substantial acidic waste, and pose challenges for safe scale-up[31-32]. Several eco-friendly reported methods such as metal-catalyzed nitration and featuring solid acid catalysts like $Fe(NO)_3$. This methods shows nitration at milder conditions with diminished environmental effects[33-35]. Numorous other metals, including Fe, Mn, Ce, Cu, and Pd, have been successfully employed for selective nitration, substitution, and transformation. This protocol offering improved safety, selectivity, and recyclability compared with conventional methods [36-40].

This is the first green approach using novel nano catalyst Cu/Mo/SiO_2 for regioselective aromatic nitration. The development of such catalysts holds great potential for improving reaction efficiency and sustainability. A relevant example illustrating the need for safer nitration strategies is the synthesis of 1-(4,5-

dimethoxy-2-nitrophenyl)ethan-1-one (2). This crucial intermediate used in the production of Cabozantinib[41]. A tyrosine kinase inhibitor used for treating various cancers, including medullary thyroid carcinoma, renal cell carcinoma, and hepatocellular carcinoma [42-44]. The conventional synthesis of this intermediate relies on nitration with fuming nitric and sulphuric acids. This process is exothermic, hazardous, and resulted in ~ 40–50% yield. 1-(4,5-dimethoxy-2-nitrophenyl)ethan-1-one (2) is highly potential intermediate for the commercialisation of Cabozantinib[45]. In addition, mechanochemical approach is employing solvent-free, $NaBH_4$-assisted synthesis of oxygen-deficient $NiCoMoO_4$ have been demonstrated significantlly[46] . Furfural Synthesised by selective oxidation of Maleic anhydride using Molybdenum/Vanadium mole ratio of catalyst[47]. Molybdenum Nano catalyst used for various transformation like oxidation, reduction and Nitrogen fixation [48-50].

In this study, we reported the efficiant, green synthesis of novel nanocatalyst $Cu/Mo/SiO_2$ via a sol–gel method. Application of this novel nanocatalyst in the nitration of aromatic compounds under mild conditions using aqueous nitric acid (fig1). To the best of our knowledge, this the first report for direct aromatic nitration under these conditions under mild, eco-friendly, green conditions using novel nanocatalyst $Cu/Mo/SiO_2$. The present protocol eliminated the use of corrosive mixed acid, and hazarodous chemicals. This proctocol shows good to excellent yields.. This methodology is a promising and sustainable strategy for green aromatic nitration reactions to producr regio selective nitrated products in a good to excellent yields.

2. Materials and Methods

2.1 Materials

Unless otherwise stated, all chemicals and solvents were of analytical grade and were used without further purification. Ethylsilicate-40 (CAS No. 18954-71-7), copper(II) acetate (Cas no.6046-93-1) sigma Aldrich 98%, ammonium heptamolybdate tetrahydrate (Cas no.12054-85-2) Sigma Aldrich grade, and isopropyl alcohol (Cas no.67-63-0) were purchased from Sigma-Aldrich. Deionized water was used throughout the catalyst synthesis. Prior to use, all glassware and reaction vessels were thoroughly cleaned, dried, and maintained under ambient laboratory conditions.

The progress of the reaction was monitored by thin-layer chromatography (TLC) using Merck silica gel 60 F_{254} precoated aluminium plates (0.2 mm thick). The chromatograms were visualized under ultraviolet light (254 nm) and, when required, by staining with phosphomolybdic acid solution in ethyl alcohol. Purification of reaction products was performed by column chromatography using activated neutral alumina or silica gel (100–200 mesh) with ethyl acetate/n-hexane as the eluent.

Nuclear magnetic resonance (NMR) spectra were recorded on a Bruker AMX-400 spectrometer operating at 400 MHz for ^1H NMR and 101 MHz for 13C NMR using $CDCl_3$ as the solvent unless otherwise specified. Chemical shifts (δ) are reported in parts per million (ppm) relative to tetramethylsilane (TMS) as the internal reference, while coupling constants (J) are expressed in hertz (Hz). Signal multiplicities are designated as s (singlet), d (doublet), t (triplet), q (quartet), dd (doublet of doublets), ddd (doublet of doublets), dt (doublet of triplets), and m (multiplet).

The present investigation showed the synthesis of novel nanocatalyst $Cu/Mo/SiO_2$ via a sol–gel method. The evaluation of catalytic performance of $Cu/Mo/SiO_2$ for the nitration reaction of a variety of aromatic substrates. The developed methodology was designed to provide a robust, economical, and environmentally benign alternative to conventional aromatic nitration.

2.2. Methods

Synthesis of $Cu/Mo/SiO_2$ Nanocatalysts

$Cu/Mo/SiO_2$ nanocatalysts were synthesised by a modified sol–gel method to obtain homogeneous dispersion of the active metal oxides.This catalyst is bound with silica matrix preserving with high surface area and structural stability. Ethylsilicate-40 was selected as the silica precursor because of its high silica content.

In a typical preparation, ethylsilicate-40 (250 g) was dissolved in anhydrous isopropyl alcohol (250 mL) under continuous magnetic stirring. Separately, cupric acetate monohydrate (12.55 g) was dissolved in isopropyl alcohol (100 mL).The resulting solution was added dropwise to the silica precursor under vigorous stirring to ensure uniform incorporation of the copper species. Ammonium heptamolybdate tetrahydrate (20.31 g) was subsequently dissolved in deionised water (100 mL) and added gradually to the reaction mixture with continuous stirring. The mixture was stirred until a homogeneous viscous sol was obtained, followed by continued stirring for an additional 2 h to facilitate gel formation.

The resulting gel was aged overnight at room temperature to promote completion of the hydrolysis and condensation reactions. The aged gel was initially air-dried and subsequently dried in a hot-air oven at 110 °C for 12 h to remove residual solvent and moisture. The dried material was then calcined in a muffle furnace at 450 °C for 12 h to obtain the final $Cu/Mo/SiO_2$ nanocatalyst.

The sol–gel synthesis produced a mechanically stable mixed-metal oxide catalyst.The homogeneous dispersion of Cu and Mo species throughout the silica framework. Subsequent structural, morphological, and compositional characterisation confirmed the successful formation of thermally stable nanostructured $Cu/Mo/SiO_2$ catalysts suitable for heterogeneous catalytic applications.

In Fig. 1 Aromatic nitration of API intermediates using hazardous fuming nitric acid, subsequent steps produced anti-cancer API Cabozantinib. By using a nano catalyst, it is easier production of advanced API

intermediates.

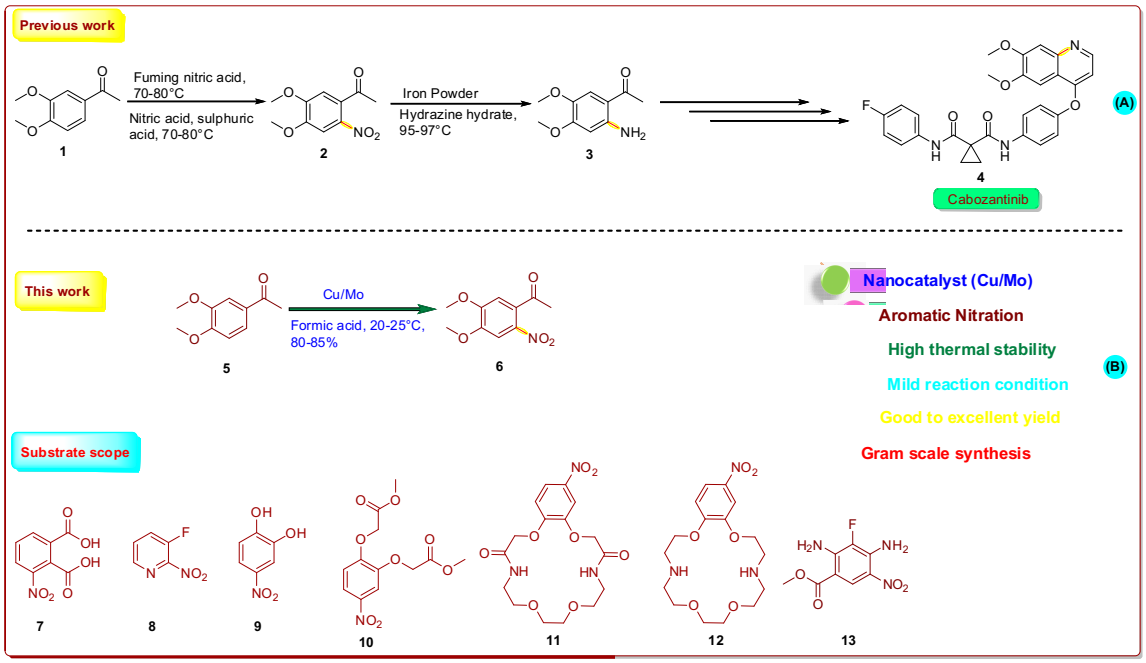
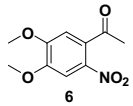
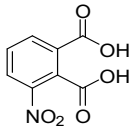
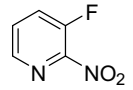
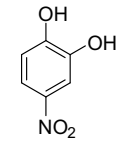
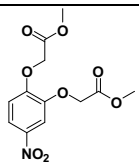
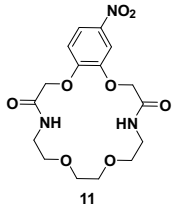
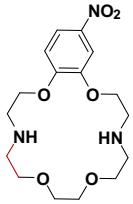
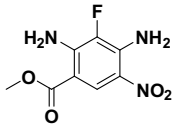


Fig.1 Aromatic Nitration of API Intermediates by using Cu/Mo/SiO_2 Catalyst.

*Nitration done by using nano Catalyst different substrates.

Table 1 Substrate Scope

Sr.N.	Product	Temp. °C	Nitration System	Time (h)	Regio isomer	Yield(%)
1.	 6	25-30°C	HNO_3/Formic acid	0.5	NA	80%
2.	 7	25-30°C	HNO_3/Formic acid	1.0	0.5	80.2%
3	 8	25-30°C	HNO_3/Formic acid	2.0	NA	65%
4	 9	25-30°C	HNO_3/Formic acid	1.5	NA	85%
5	 10	25-30°C	HNO_3/Formic acid	2.5	0.61	81%

6	 11	25-30°C	HNO_3/Formic acid	3.0	NA	89%
7	 12	25-30°C	HNO_3/Formic acid	3.5	NA	86%
8	 13	25-30°C	HNO_3/Formic acid	1.5	NA	83%

All compounds synthesis data have been included in supporting information

The above table 1 substrate used for the synthesis of active pharmaceutical ingredients has higher worldwide consumption.

The optimisation of 3-nitrophthalic acid synthesis under various reaction conditions is presented in Table 2. The results indicate that the current catalytic system affords the desired regioisomer with minimal formation of other regioisomeric products.

Table 2. Reaction carried out different weight % Of catalyst loading details table

Sr.N.	Comp.no.	Catalyst Loading (%)	HNO_3 (eq.)	HCOOH (V) (Solvent+Reagent)	Temp	Conversion	Regio isomer (4-Nitro)	Yield
1	7	NA	1.99	5.0	25-30°C	NA	NA	NA
2	7	NA	1.99	5.0	50-55°C	NA	NA	NA
3	7	NA	1.99	5.0	100-105°C	NA	NA	NA
4	7	5	1.99	5.0	25-30°C	55%	0.05%	45%
5	7	5	1.99	5.0	45-50°C	60.7%	0.05%	46%
6	7	5	1.99	5.0	100-105°C	67.7%	0.1%	51%
7	7	7	1.99	5.0	25-30°C	56%	0.04%	47%
8	7	7	1.99	5.0	45-50°C	60.7%	0.45%	55%
9	7	7	1.99	5.0	100-110°C	75.7%	1.55%	65%
10	7	7	1.99	5.0	25-30°C	85%	0.55%	79.5%
11	7	10	1.99	5.0	45-50°C	90%	3.8%	80.10%
12	7	10	1.99	5.0	100°C	65%	30%	45 %
13	7	10%	1.99	5.0	25-30°C	85.8%	0.5%	80.2%

*Yield is calculated on an isolated basis. The reaction was done on a 100 gm scale basis.10% catalyst loading, 100% product degradation observed and Regioisomer formation observed, to controlled regio isomer at 25 to 30°C at the best condition.

2.3 Experimental

We commenced our investigation by evaluating the reaction of formic acid with aqueous nitric acid (60–70%) in the presence of the Nano catalyst (10 g, 10% w/w). Nitric acid was used as nitrating agent to introduce nitro functional group. While formic acid served as the solvent and provide acidic medium required for nitration. To this nitrating mixture, 1-(3,4-dimethoxyphenyl)ethan-1-one (5) was added at ambient temperature and stirred for 30 min. As anticipated, the desired product, 1-(4,5-dimethoxy-2-nitrophenyl)ethan-1-one (6), was obtained with 80% yield.

It was further observed that substituents exert a pronounced electronic effect on the phenol ring. Substrates bearing electron-withdrawing groups, such as diacids, furnished significantly higher yields (7) compared to those containing electron-donating substituents (-OH, -OR, -NH_2). This trend highlights the favourable role of electron-withdrawing groups in facilitating the transformation. Gratifyingly, a mono-substituted halogen (-F) heteroaromatic system, exemplified by 3-fluoropyridine, afforded the corresponding product (8) in excellent yield (65%). Nitration of 3-fluropyridine is not reported in any literature, but a product is prepared using hazardous tetrafluoro acid[51]. Our catalytic system is favourable for this conversion, further emphasising the importance of electronic factors. In contrast, electron-donating substituents delivered compounds 9 and 10 at moderate to excellent yields (69% and 96%, respectively), indicating that although donation tends to reduce reactivity, efficient conversion is still achievable. Interestingly, sterically hindered bicyclic aromatic systems also furnished compounds 11 and 12 with high yields (91% and 93%). This clearly suggests that steric hindrance has minimal influence on the efficiency of this transformation, underscoring both the robustness and broad substrate tolerance of the methodology.

Reaction Mechanism:-

Figure 2 illustrates the complete reaction mechanism for aromatic nitration using the nanocatalyst.

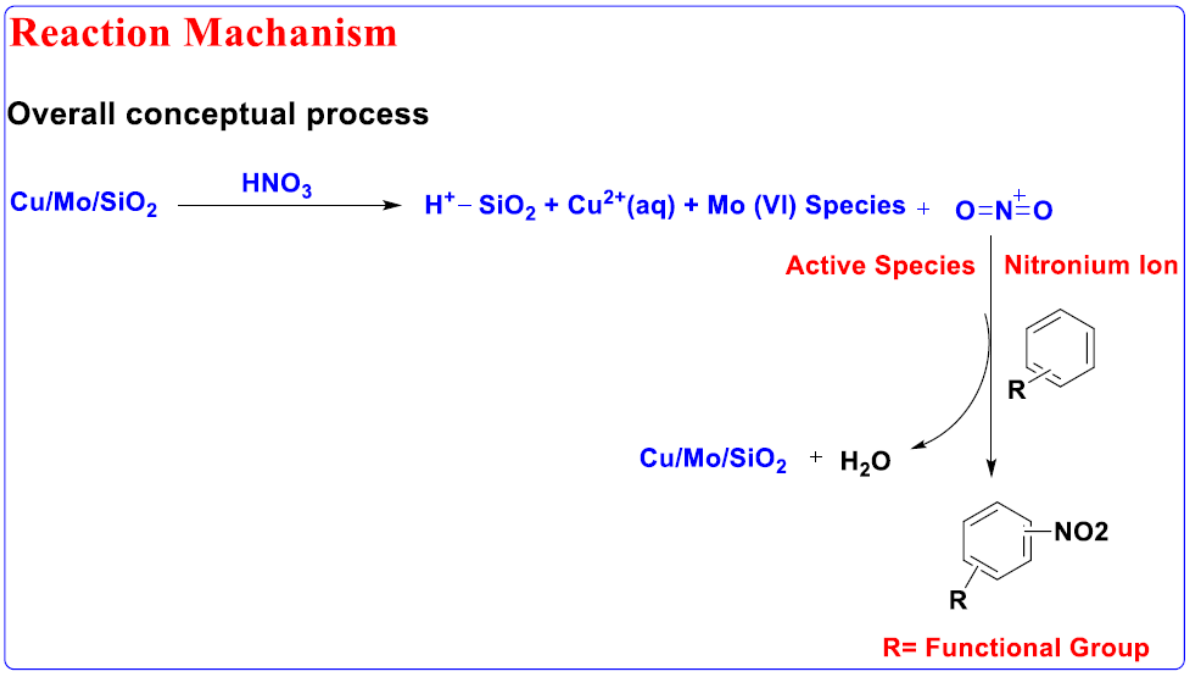


Fig. 2 Reaction mechanism by using Nano-catalyst.

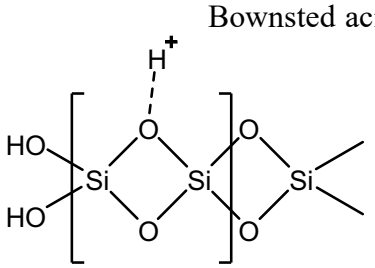
Attack of HNO_3

The mobile metal atoms Cu and Mo embedded in the porous framework are selectively oxidised by incoming HNO_3. This alters their chemical state from neutral to positive, which has high affinity for water and immediately floats out into the liquid phase Cu^{2+}(aq.) and soluble Mo(IV) species.

(SiO_2)-M(o)+ $4HNO_3$+$4H^+$ ⟶ Mo^{4+} +$4NO_2$+ $4H_2O$

Framework Activation

Once the heavy metal are removed, the exposed oxygen lone pair on the silica backbone rapidly absorbs excess protons from the conch. Acid pool. This converts into a passive silica mixture into an activated ‘’Bronsted solid acid.’



Catalytic Dehydration

The heavily protected silica matrix interacts with unreacted HNO3. It forces the transfer of an additional hydrogen on the acid molecule, driving a dehydration split to expel water and leave behind the stable linear electrophile, i.e. Nitronium Ion.

$$\left[\ H_2O\text{-}NO^2\ \right] \longrightarrow H_2O + \overset{+}{N}O_2$$

Cu–Mo–Si nano catalysts enable efficient, and eco-friendly aromatic nitration using aqueous nitric acid under mild conditions.

3.0 Result and Discussion

3. X-ray Diffraction (XRD) Analysis

The XRD patterns of 10 wt.% Cu/Mo/SiO2 (CMS) catalysts, calcined at various temperatures from 500 °C to 700 °C, are shown in Fig. 3. The catalysts were synthesised via solgel technique to ensure uniform metal dispersion on silica[52]. Distinct diffraction peaks at 2θ = 12.7°, 23.3°, 25.8°, and 27.3° correspond to orthorhombic α-MoO3 phase (JCPDS No. 00-005-0508). No β-MoO3 signals appeared, consistent with its thermal instability above ~400 °C. XRD patterns with varying copper loadings (0.5%, 5%, and 10%) confirmed retention of α-MoO3 across compositions[53-55]. At 10 wt.% Cu, additional reflections at 2θ = 35.7° and 46.3°, assigned to monoclinic CEO phase .

Increasing dopant concentration led to minor shifts in peak intensity and broadening, indicating changes in crystallinity and reduced average crystallite size. The Scherrer equation calculations revealed a slight decrease in crystallite size with increasing calcination temperature, suggesting the formation of thermally stable nanocrystalline phases [56-59].

Calcination at 600 °C and 700 °C produced XRD patterns similar to those at 500 °C, confirming the thermal stability of both α-MoO_3 and CuO phases. [59] These results demonstrate that the CMS catalysts possess robust crystalline structures suitable for high-temperature catalytic applications, with Cu and MoO_3 components remaining stable under thermal stress[60].

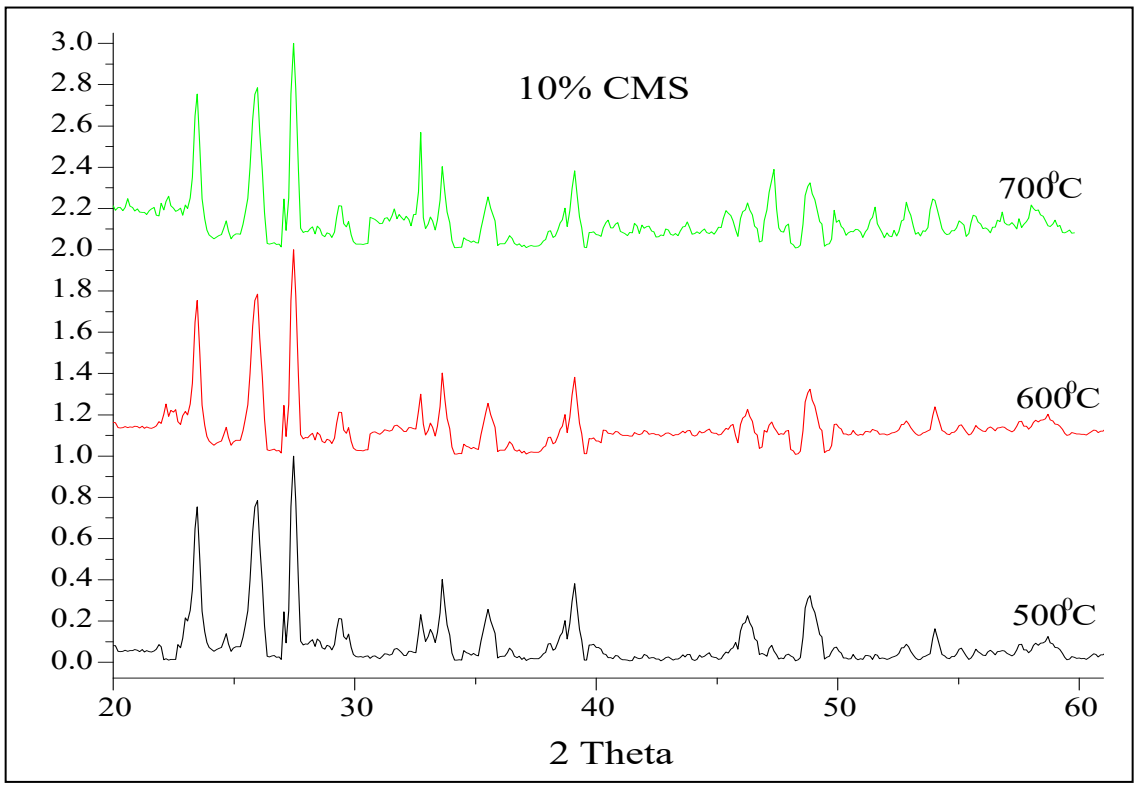


Figure-3. Comparative XRD Graph 10% Cu/Mo/SiO_2 at various calcined temperature

(P) XRD pattern of Cu (10 wt.%)/Mo/ SiO_2 contains: a) MoO_3 phase at 12.8⁰,23.8⁰, 26.9⁰; b) CuO – 35.7⁰, 46.3⁰. In the above Fig shows characteristic diffraction peak of Cu/Mo/SiO_2 nanocatalyst. The peaks observed at 2θ values of 12.8°, 23.8°, and 26.9° are attributed to the crystalline phase of MoO while the peaks at 35.7° and 46.3° are associated with CuO. These diffraction peaks indicate the formation of crystalline metal oxide phases within the nanocatalyst, providing structural information relevant to its further characterisation and evaluation of catalytic performance.

3.2 Scanning Electron Microscopy (SEM) and Energy Dispersive X-ray (EDX) Analysis

The surface morphology and elemental distribution of the synthesised mixed metal oxide catalysts were studied using scanning electron microscopy (SEM) and energy dispersive X-ray (EDX) spectroscopy **(Figure-4)**. Representative SEM micrographs along with corresponding EDX spectra are shown in **Figure-4 &**

5. SEM analysis revealed that the catalysts exhibit well-defined, granular or cubic-like morphologies with relatively uniform particle size distribution. The nanostructured surfaces indicate efficient incorporation of metal precursors into the silica matrix via the sol–gel route, suggesting good dispersion of active components without significant aggregation.[61-62].

EDX spectra confirmed the presence of the desired metal species in the silica framework. Elemental analysis clearly showed Cu, Mo, and Si in Cu/Mo/SiO_2 catalysts. The absence of extraneous elements validated the high purity and targeted stoichiometry of the synthesised materials. [63-65]. The uniform distribution of elements supports the potential of these catalysts for consistent and reproducible catalytic performance[66-67].

SEM and EDX analyses together confirm that the sol–gel synthesis yields homogeneous, nanoscale mixed oxide catalysts with desirable surface characteristics and compositional accuracy, critical for catalytic activity and stability.

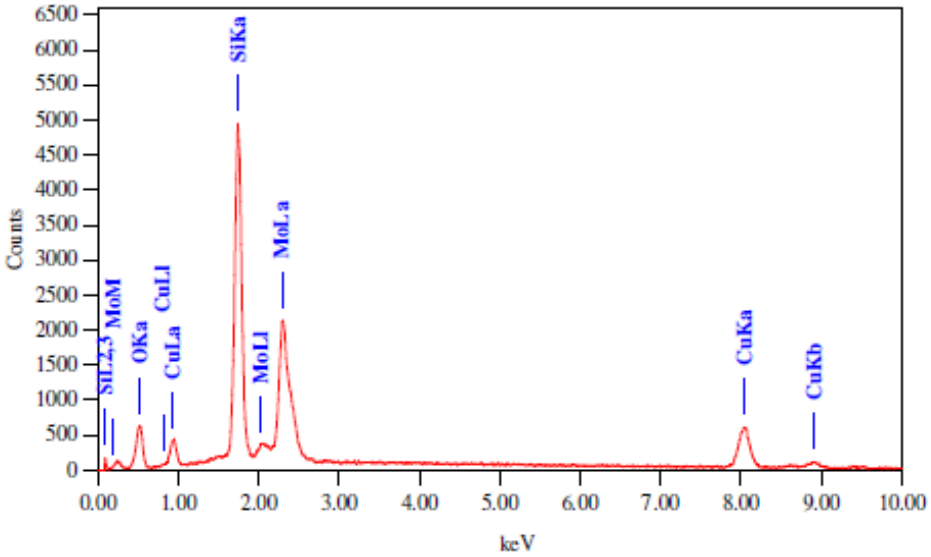


Figure-4. Energy Dispersive X-ray (EDX)

In the EDX analysis, it clearly indicated that elemental species present in molecules, the different peaks show that peaks like Si, Cu, Mo, which clearly understand the elemental species present in the nano-structure characteristic X-ray energies (keV) on the x-axis to specific electronic transitions.

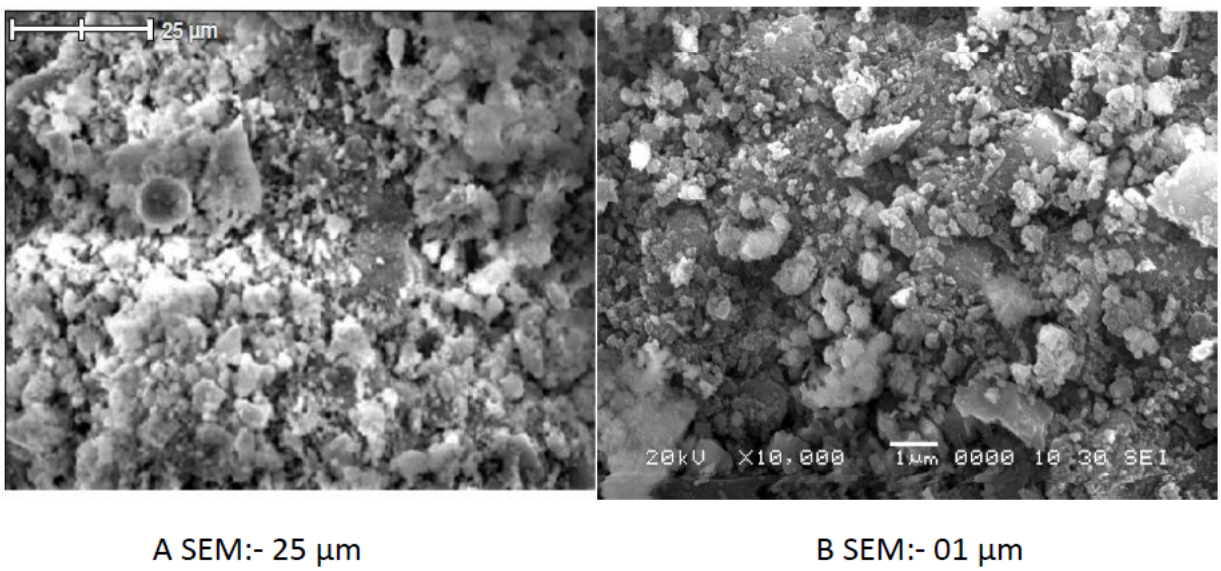


Figure-5. SEM micrographs 10%- Cu/Mo/SiO_2 500°C

Scanning Electron Microscopy (SEM) analysis showing surface images, which is clearly indicated the surface size of a nano-particle[35]. SEM is Surface analysis method. From this method we will analyse the surface structure of the nano-particle, which will help for further studies.

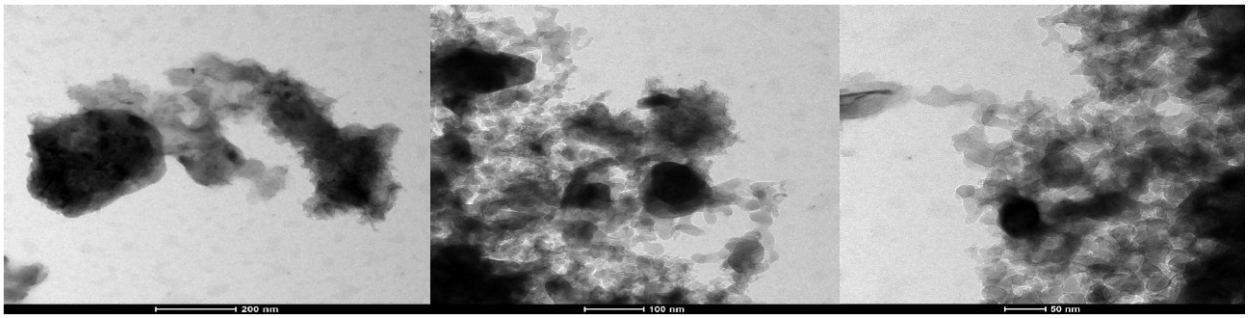
The images show microstructure, morphology, and surface characteristics. SEM images of a 10% Cu/Mo/Si bimetallic nano catalyst showing constant size globular morphology used for various organometallics' reaction as per globular morphology are very useful.

3.3 Transmission Electron Microscopy (TEM) Analysis

Transmission electron microscopy (TEM) was employed to investigate the particle size, morphology, and nanostructure of the synthesized catalysts[68]. Representative TEM images of MoO_3 and 10 wt.% Cu/Mo/SiO2 are shown in Fig. 6. The TEM micrographs reveal nanocrystalline structures with rectangular to slightly irregular nanoparticles[69]. These particles tend to form agglomerates, commonly seen in nanostructured oxides due to high surface energy. The contrast between metal oxide particles and silica support allowed visualization and measurement of particle sizes, which were found to be 20–30 nm, confirming the nanoscale nature of the active phase.

These size estimates align with crystallite sizes calculated from XRD peak broadening using the Scherzer equation, validating the consistency between characterisation techniques[70-73]. TEM analysis corroborates the high dispersion of metal species on the silica matrix and confirms the successful synthesis of well-dispersed nanostructured catalysts via the sol–gel route.

The structural integrity and uniform morphology observed by TEM indicate potential high surface area and accessible active sites, which are crucial for enhanced catalytic activity [74-76].



A:- TEM 200 nm B:- TEM 100 nm C:- TEM 50 nm

Figure-6. TEM micrographs **10%- Cu/Mo/SiO_2 500°C.**

Transmission Electron Microscopy (TEM) is a high-resolution imaging technique used to distinguish nanoparticles by transferring an elevated-energy electron beam through ultra-thin samples.[36]It provides direct, sub-nanometer visualisation of particle morphology, exact size, size distribution, crystal structure, and lattice orientation. TEM provides 2D projection of nano-particles. It shows the internal structure of nano particles like species, rodlike, polyhedral. In the above fig. it shows the internal structure of a Cu/Mo/Si nano particle, which shows a particle size of 20 nm to 30nm. The images confirmed the formation of spherical morphology. The average particle size obtained from TEM was found to be in the range 20–30 nm, which is in good agreement with results obtained by XRD.

3.4 General Procedure for Synthesis of Compounds 6-12

1-(4,5-Dimethoxy-2-nitrophenyl)ethan-1-one (6)

To a solution of formic acid (500 mL) was added aqueous nitric acid (60–70%, 83.89 g, 1.33 mol), and the mixture was stirred for 10–15 min. Subsequently, Nano catalyst (10 g, 10% w/w) was added. To this nitrating mixture, 1-(3,4-dimethoxyphenyl)ethan-1-one (100.0 g, 0.54 mol) was added in five equal portions at 30 °C while maintaining the reaction temperature between 25–30 °C. After 30 min, TLC indicated completion of the reaction. The reaction mixture was diluted with water (500 mL) and stirred for 45–60 min. The product was extracted with dichloromethane (3 × 300 mL). The combined organic layers were dried and concentrated under reduced pressure to afford 90 g of white crystalline solid in 80% yield. The purity was confirmed to be 98.3% by HPLC.

^{1}H NMR (400 MHz, DMSO-d_6, δ ppm): 2.50 (s, 3H), 3.89 (s, 3H), 3.92 (s, 3H), 7.20 (s, 1H), 7.63 (s, 1H). **^{13}C NMR** (100 MHz, DMSO-d_6, δ ppm): 107.10, 109.65, 131.12, 138.34, 149.34, 153.12, 199.30. **ESI-MS** (m/z): $[M+H]^+$ calcd. for: $C_{10}H_{12}NO_5$: 226, found: 226.

3-Nitrophthalic Acid (7)

To a solution of formic acid (500 mL) was added aqueous nitric acid (60–70%, 291 g, 2.07 mol), and the mixture was stirred for 10–15 min. A nano catalyst (10 g, 10% w/w) was then added. To this nitrating mixture, phthalic acid (100.0 g, 1.04 mol) was added and stirred at 25–30 °C. After 30 min, TLC confirmed completion of the reaction. The reaction mass was diluted with water (3 × 500 mL) and stirred for 45–60 min. The product was extracted with dichloromethane (3 × 500 mL), and the combined organic layer was concentrated under reduced pressure to afford a crude oily product. The pure product was obtained by high vacuum distillation (yellow oil), which solidified upon standing overnight. Final distillation was carried out at 70–72 °C

under 8–9 mm Hg to yield 100 g of 3-nitrophthalic acid in 78% yield. HPLC purity was found to be 99.5%.
^{1}H NMR (400 MHz, DMSO-d_6, δ ppm): 7.50 (t, 2H), 8.50 (m, 2H). **^{13}C NMR** (100 MHz, DMSO-d_6, δ ppm): 116.69, 116.92, 126.53, 126.53. **ESI-MS** (m/z): $[M+H]^+$ calcd. for: $C_8H_6NO_6$: 212, found: 212

3-Fluoro-2-nitropyridine (8)
To a solution of formic acid (400 mL) was added aqueous nitric acid (60–70%, 108 g, 0.77 mol), and the mixture was stirred for 10–15 min. Nano catalyst (10 g, 10% w/w) was then added. To this nitrating mixture, 3-fluoropyridine (100.0 g, 0.38 mol) was added and the reaction was stirred at 25–30 °C. After 30 min, TLC confirmed completion of the reaction.
The reaction mixture was diluted with water (3 × 500 mL) and stirred for 45–60 min. The product was extracted with dichloromethane (3 × 500 mL), and the combined organic layers were concentrated under reduced pressure to afford the crude product. The crude compound was stirred in n-hexane for 2 h at 25–30 °C to induce crystallization. After filtration, 100 g of the solid product was obtained in 65% yield. HPLC purity was found to be 98.6%. **^{1}H NMR** (400 MHz, DMSO-d_6, δ ppm): 7.7(m, 1H),7.8(t, 1H), 3.82 (s, 1H), **^{13}C NMR** (100 MHz, DMSO-d_6, δ ppm): 128.32,130.50,143.90,150.32,153.06. **ESI-MS** (m/z): $[M+H]^+$ calcd. for: $C_5H_4FN_2O_2$: 143, found: 143.
The following compounds are also prepared by the same general procedure as mentioned above.
4-nitrobenzene-1,2-diol (9)
^{1}H NMR (400 MHz, DMSO-d_6, δ ppm): 6.88-6.90 (d, 1H), 7.59-7.60 (d, 1H), 7.62-7.65 (dd, 1H), 10.00 (s, 1H), 10.55 (s, 1H). **ESI-MS** (m/z): $[M+H]^+$ calcd. for: $C_6H_6NO_4$: 156, found: 156

Dimethyl 2,2'-((4-nitro-1,2-phenylene)bis(oxy))diacetate (10)
^{1}H NMR (400 MHz, DMSO-d_6, δ ppm): 5.02-5.04 (s, 4H), 3.71-3.72 (s, 6H), 7.15-7.17 (d, 1H), 7.75-7.76 (d, 1H), 7.88-7.91 (dd, 1H). **ESI-MS** (m/z): $[M+H]^+$ calcd. for: $C_{12}H_{14}NO_8$: 300, found: 300
18-nitro-5,6,8,9,12,13-hexahydro-2H,11H-benzo[b][1,4,10,13]tetraoxa[7,16]diazacyclooctadecine-3,14(4H,15H)-dione (11)
^{1}H NMR (400 MHz, DMSO-d_6, δ ppm): 3.33-3.38 (m, 4H), 3.48 (m, 8H), 7.28-7.31 (s, 1H), 7.87-7.96 (m, 4H). **ESI-MS** (m/z): $[M+H]^+$ calcd. for: $C_{16}H_{22}N_3O_8$: 384, found: 384

18-Nitro-3,4,5,6,8,9,12,13,14,15-decahydro-2H,11H-1,7,10,16,4,13-benzotetraoxadiazacyclooctadecine (12). Nature - yellow solid (1.120 g, 86% yield). ^{1}HNMR (400 MHz, $CDCl_3$) δ 2.25 (s, 2H, NH), 2.86 (t, *J = 4.6 Hz*, 3.07 (t, *J = 4.6 Hz*, 4H),4H), 3.60 (s, 4H), 3.63 (m, 4H), 4.19 (m, 4H), 6.87 (d, *J = 9.0 Hz,* 1H,), 7.71 (d, *J = 2.6 Hz*, 1H), 7.87 (dd, *J = 9.0*, 2.6 Hz, 1H). ^{13}CNMR (126 MHz, CDCl3) δ 48.43, 48.46, 49.43, 49.47, 68.77, 69.14, 70.39, 70.44, 70.48, 106.88, 110.33, 117.73, 141.35, 148.34, 154.13 ppm. **ESI-MS** (m/z): $[M+H]^+$ calcd. for: $C_{16}H_{25}N_3O_6$: 356.180 ([M+H]+, Calcd; 356.181).
Methyl 2,4-diamino-3-fluoro-5-nitrobenzoate (13) Nature- Light yellow solid (95% Yield) ^{1}HNMR (400 MHz, DMSO) δ 3.81 (s,3H,-0CH_3), δ 7.21 (s,2H,-NH_2), δ 7.37 (s,2H,-NH_2),
δ 8.54 (s,1H,-CH), ^{13}CNMR (100 MHz, CDCl3) δ 101,123,126,135,137,138,142,166 ppm. **ESI-MS** (m/z): $[M+H]^+$ calcd. for: $C_8H_8FN_3O_4$: 229.2 ([M+H]+, Calcd; 229.21).

Above all, compounds are synthesized using Cu/Mo/Si Nano-particles with aq. Nitric acid, which in this methodology, the nano-particle, helps to speed up the reaction within a stipulated time with a robust process, eco-friendly, no hazardous reagents like fuming nitric acid, sulphuric acid involved, temp not requiring more than 35°C, reaction completed at ambient temp, isolation very simple by filtration or extraction, catalyst recovery done by precipitation.

4. Conclusions
Novel nanostructured Cu/Mo/SiO2 catalysts were synthesised via the sol–gel method and effectively applied for aromatic nitration using aqueous nitric acid under mild conditions. The process delivered excellent yields with short reaction times and simple product isolation, eliminating the need for corrosive acids. This green, cost-effective method is industrially safe and suitable for synthesising key API intermediates. The catalysts demonstrated good thermal stability and scalability, making them promising for pharmaceutical and fine chemical applications. Overall, this work represents a significant step toward sustainable, heterogeneous catalytic systems for aromatic nitration. Although promosing result of novel nanocatalyst $Cu/Mo/SiO_2$ has certain limitations, however its production of nanocatalyst by solgel method having current challenges in maintaining defined/uniform structure, composition, porosity, and catalytic activity during commercial batches.

5. List of Abbreviations
Ar = Aryl; DMSO = Dimethyl sulfoxide; FT-IR = Fourier transform infrared spectroscopy; FWHM = Full width at half maximum; ICP-AES = Inductively coupled plasma atomic emission spectroscopy; MP = Melting point; NMR = Nuclear magnetic resonance; NPs = Nanoparticles; Ph = Phenyl; ppm = Parts per million; RBF = Round-bottom flask; RT = Room temperature; SEM = Scanning electron microscopy; TEM = Transmission electron microscopy; THF = Tetrahydrofuran; TLC = Thin-layer chromatography; TMS = Tetramethyl silane; UV–Vis = Ultraviolet–visible spectroscopy; VSM = Vibrating sample magnetometry; XRD = X-ray diffraction.

6.Declarations
Ethics Approval and Consent to Participate this study involved only chemical synthesis, catalyst preparation,

physicochemical characterization, and evaluation of chemical reactions. No human participants, animals, human tissues, or biological samples were involved. Therefore, ethics committee or institutional review board approval was not required.

7. Acknowledgment

DP gratefully acknowledges the financial support from Bharati Vidyapeeth (Deemed to be University), Y.M. College, Pune, and INFINIA Sciences, Pune, India.

8. Author Contributions

Study conception and design by Suras Mohite and Sathiyanarayanan Lohidasan, data collection by Sharada Gadale, analysis and interpretation of results by Devidas B. Patil, and draft manuscript done by Aarif Shaikh. All authors reviewed the results and approved the final version of the manuscript.

9. Conflict of interest

The authors declare that there are no competing financial or non-financial interests associated with this work.

References

[1] Neele Puhlmann,;Rodrigo Vidauree,;Klauss Kummer, Designing greener active pharmaceutical ingredients: Insights from pharmaceutical industry into drug discovery and development, *European Journal of Pharmaceutical Sciences* **2024**,*192*, 106614, 10.1016/j.ejps.2023.106614.

[2] Vishal Shah, Manufacturing of Clinical Active Pharmaceutical Ingredients: Process Design, Scale-Up, and Control of Multi-Step Chemical Synthesis, *Int. J. of Pharm. Sci.*, **2026**, 4(4), 3020-3031, 10.5281/zenodo.19660715.

[3] Nico Fleck,Frank Roschangar,Alexander M. Haydl; API Syntheses in Aqueous Media: Assessing the Environmental Footprint en route from Academic Discovery to Industrial Applications as Green Opportunity for Process Chemistry,*Org. Process Res. Dev*.,**2023**,27 (5),822,830.,10.1021/acs.oprd.3c00037.

[4] Khan, M. A. A., & Rauf, A. (2024). Promoting local production and active pharmaceutical ingredient (API) industry in low- and middle-income countries (LMICs): impact on medicines access and policy. *Journal of Pharmaceutical Policy and Practice*, **2024**,17(1).,10.1080/20523211.2024.2323683

[5] Bruce Lipshutz,; Sachin Handa,; Modernizing the 12 principles of green chemistry: it's time, *Green Chem.* **2026**, *28*(*13*): 5606–5612, 10.1039/d5gc05289k.

[6] Francesca M. Kerton, Applying the principles of green chemistry to achieve a more sustainable polymer life cycle*, Current Opinion in Green and Sustainable Chemistry*, **2025**,51,100996,2452-2236, 10.1016/j.cogsc.2024.100996.

[7] Gunjan Arora,; Ruchi Shrivastava.; Prashant Kumar,; Rakeshwar Bandichhor.; Dileep Krishnamurthy,; Rakesh Kumar Sharma,; Avtar S. Matharu,; Jaya Pandey.; Recent advances made in the synthesis of small drug molecules for clinical applications: an insight *Current Research Green and* Sustainable *Chemistry*.,**2021**,4, 2666-2865,10.1016/j.crgsc.2021.100097

[8] A Review of Industrial Applications of Green Chemistry: Review Article, *Journal of Pharma Insights and Research*, **2025**,*3*(1), 186-196. https://doi.org/10.69613/der2my50.

[9] Sageer Ahmad,; Rahul Jaiswal,; Reetu Yadav,; Sarita Verma. Recent advances in green chemistry approaches for pharmaceutical synthesis, *Sustainable Chemistry One World*, **2024**, (4),100029, 10.1016/j.scowo.2024.100029.

[10] Stefanache, A.; Marcinschi, A.; Marin, G.-A.; Mitran, A.-M.; Lungu, I.I.; Miftode, A.M.; Crivoi, F.; Lacatusu, D.; Baican, M.; Cioanca, O.; et al. Green Chemistry Approaches in Pharmaceutical Synthesis: Sustainable Methods for Drug Development. *Applied Chem* **2025**, *5*, (13).,10.3390/appliedchem5020013.

[11] C. V. A. Sasikala, P. D. Nahide, A. Srivastava, S. Dutta, R. K. Sharma, and R. Bandichhor, in The Business Case for Green Chemistry, ed. G. A. Hurst and J. H. Clark, Royal Society of Chemistry, 2026, vol. 91, ch. 6, pp. 144-186. https://doi.org/10.1039/9781837673490-00144.

[12] Rao, C. N. R.,Green Chemistry Approaches to the Synthesis of Pharmaceutical Intermediates: Minimizing Environmental Impact. *Modern Dynamics Journal of Chemistry (MDJC)*, **2024**,1(1), 1–6.,10.36676/mdjc.v1.i1.1.

[13] Mohit Mishra, Mansi Sharma, Ragini Dubey, Pooja Kumari, Vikas Ranjan, Jaya Pandey, Green synthesis interventions of pharmaceutical industries for sustainable development, Current Research in *Green and Sustainable Chemistry*, **2021,** 4,100174, https://doi.org/10.1016/j.crgsc.2021.100174.

[14] Kuyucu, A.E., Selçuk, A., Önal, Y. *et al.* Sustainable synthesis and characterization of high-surface-area activated carbons from walnut and pistachio shell wastes via chemical activation. *Sci Rep* **2026**,16, 12776, 10.1038/s41598-026-43746-8.

[15] Rahina Mohammad Kunhi, Jishina Karunakaran, Rashmi Kunhiraman, Manjunatha Pattabi, Nanditha Thayyath Kizhakkeveettil, Rani Manjunatha Pattabi, Gurumurthy Sangam Chandrasekhar; Reductive Stability of Organic Dyes in Nano catalyst-Assisted Sodium Borohydride Systems. *ACS Omega*,**2026**,11 (19), 28569–28581. 10.1021/acsomega.6c00189.

[16] Weichen Zhao, Muhammad Adeel, Peng Zhang, Pingfan Zhou, Lili Huang, Yongwen Zhao, Muhammad Arslan Ahmad, Noman Shakoor, Benzhen Lou, Yaqi Jiang, Iseult Lynch, Yukui Rui; A critical review on surface-modified nano-catalyst application for the photocatalytic degradation of volatile organic compounds. *Environ. Sci.: Nano* **2022**; 9 (1): 61–

80., 10.1039/d1en00955a.
[17] Hasan Ahmad, Mohammad Kawsar Hossain; Supported nanocatalysts: recent developments in microwave synthesis for application in heterogeneous catalysis. *Mater. Adv.* **2022**; 3 (2): 859–887. https://doi.org/10.1039/d1ma00840d.
[18] Yeom J,; Lorenzin G,; Ghisalberti L,; Cancellieri C,; Janczak-Rusch J, The thermal stability and degradation mechanism of Cu/Mo nano multilayers. *Sci Technol Adv Mater*. **2024** ;25(1):2357536. 10.1080/14686996.2024.2357536.
[19] Sharma KP,;Shin M, Awasthi GP,; Cho S, Yu C. One-step hydrothermal synthesis of CuS/MoS_2 composite for use as an electrochemical non-enzymatic glucose sensor. *Heliyon*. **2023** ,10(*2*),e23721,10.1016/j.heliyon.2023.e23721.
[20] Agatha Ifeoma Ijomah,; Kingsley Chidi Nnakwo,; Jerome Ugwu Odo,; Ifeanacho Uchenna Okeke, Improving the structure, tensile strength and hardness of molybdenum-doped copper-silicon alloy system, *International Journal of Mechanical and Industrial Technology* , **2023**,11(*1*) :10.5281/zenodo.8348223.
[21] Krisha SG, Menaka S, Celshia S, Selvamani M, Suresh V. Synthesis of Copper Molybdate and Its Electrochemical Sensing of Paracetamol. *Cureus*. **2024** ;16(7):e63925. 10.7759/cureus.63925.
[22] Maraj, M.; Raza, A.; Wang, X.; Chen, J.; Riaz, K.N.; Sun, W. Mo-Doped CuO Nanomaterial for Photocatalytic Degradation of Water Pollutants under Visible Light. *Catalysts* **2021**, *11*, 1198.,10.3390/catal11101198.
[23] Yanfang Liu, Keqin Feng, Hongling Zhou, Sitan Chen, Microstructure and phases investigations of W.Mo.Cu alloy prepared by large current electric field sintering, Intermetallics,**2022**,143, 107488, 10.1016/j.intermet.2022.107488.
[24] Jayawardena HSN, Liyanage SH, Rathnayake K, Patel U, Yan M. Analytical Methods for Characterization of Nanomaterial Surfaces. *Anal Chem*. **2021**,93(4):1889-1911. 10.1021/acs.analchem.0c05208.
[25] Aziz, A., Shaikh, H., Abbas, A., Zehra, K.E. and Javed, B. Microscopic Techniques for Nanomaterials Characterization: A Concise Review. *Microsc Res Tech*,**2025**, 88,1599-1614. 10.1002/jemt.24799.
[26] Satyam Verma, Manisha Kumari, Reetu Maurya, Kanak Roy, Recent advances in single-atom heterogeneous catalysts in thermos catalytic carbon dioxide hydrogenation to methanol, *Materials Today*,**2025**, **89,**606-620,10.1016/j.mattod.2025.08.010.
[27] Di Xu, Ning Yan, Dynamic *Heterogeneous Catalysis*,**2026**,10.1021/acsinfocus.7e9021.
[28] S. S. Patel, D. B. Patel, H. D. Patel, *Chemistry Select* **2021**, *6*, 1337, 10.1002/slct.202004695.
[29] Yanxuan Wu, Wen Lu, Yan-Na Ma, Feijing Chen, Wei Ren, Xuenian Chen; Trifluoromethanesulfonic Acid Promoted Controllable Electrophilic Aromatic Nitration. *Journal of Organic Chemistry* ,**2023**; 88 (15): 11322–11327. ,10.1021/acs.joc.3c00892.
[30] Benoit Cardinal-David, Kaid C. Harper, Anuj Verma, David Hanna, Daniel D. Caspi, Christopher Vitale, Jeffrey T. Bien, Zhe Wang, Moiz Diwan; Continuous Multiphase Flow Nitration and Cryogenic Flow Formylation: Enabling Process Development and Manufacturing of Pharmaceutical Intermediates. *Org. Process Res. Dev.* **2021**; 25 (11): 2473–2481. ,10.1021/acs.oprd.1c00249.
[31] James I. Murray, Maria V. Silva Elipe, Kyle D. Baucom, Derek B. Brown, Kyle Quasdorf, Seb Caille; *Ipso* Nitration of Aryl Boronic Acids Using Fuming Nitric Acid. *Journal of Organic Chemistry* , **2022**; 87 (4): 1977–1985. ,10.1021/acs.joc.1c00886.
[32] Haruro Ishatani,; Masahiro Sasaya,; and Shu Kobayashi, Liquid-phase Catalytic Continuous-Flow Aromatic Nitration Reactions with Conc. HNO3 on Modified Mixed-Metal Oxide Composites as High-Yielding Solid Acid Catalysts *ACS Sustainable Chem. Eng*. **2023**, 11, (15), 5826–5833. ,10.1021/acssuschemeng.2c04616
[33] Yuzhu Zheng, Qi-Qi Hu, Qing Huang, Youwei Xie; Late-Stage C–H Nitration of Unactivated Arenes by Fe(NO3)3·9H2O in Hexafluoro isopropanol. *Org. Lett*. **2024**; 26 (15): 3316–3320. ,10.1021/acs.orglett.4c01006.
[34] Yang, Xiaohan, Wang, Biqin, Zhang, Qian, Szekely, Aron, Wu, Mengxiang, Li, Yahong Nitration of Derivatives of Imidazo[1,5-a]pyridine via C−H Functionalization with Fe(NO3)3 · 9H2O as a Promoter and a Nitro Source, *Chemistry Select*, , **2024, 9**, 10.1002/slct.202401114.
[35] Yuzhu Zheng, Zongyi Liu, Qing Huang, Youwei Xie,Ipso-Nitration of Boronic Esters Enabled by Ferric Nitrate Nonahydrate (Fe(NO3)3·9H2O) in HFIP,*Organic Letters*, **2025**, 27,(12),2997-3002,10.1021/acs.orglett.5c00635.
[36] Cunluo Wu, Qilong Bian, Tao Ding, Mingming Tang, Wenkai Zhang, Yuanqing Xu, Baoying Liu, Hao Xu, Hai-Bei Li, Hua Fu; Photoinduced Iron-Catalyzed *ipso*-Nitration of Aryl Halides via Single-Electron Transfer. *ACS Catal.* **2021**; 11 (15): 9561–9568., 10.1021/acscatal.1c02272.
[37] Tiwari, M.S., Kumaran, S. and Manyar, H.G.. Metal Oxides as Catalysts/Supports in Solvent-Free Organic Reactions. In Solvent-Free Methods in Nanocatalysis (eds R. Luque, M.B. Gawande, E. Doustkhah and A. oswami) 2023,10.1002/9783527831463.ch4
[38] Kumar, V.; Dharaniyedath, J.; T P, A.; Ariyan, S.; Venkatesh, C.; Gandeepan, P. *Beilstein J. Org. Chem.* **2025**, 21, 2479–2488. doi:10.3762/bjoc.21.190.
[39] Wen-Pei Li,,Guo Cheng,Si-Yuan Li, Cheng-Zhou Lin, Xiao-Yu Guan, De-Xian Bing, Jing Cao, Di Zhu, Qing-Hai Deng; Acid-Free Copper-Catalyzed Electrophilic Nitration of Electron-Rich Arenes with Guanidine Nitrate. *Journal of Organic Chemistry*, **2022**; 87 (5): 3834-3840,https://doi.org/10.1021/acs.joc.1c03020.
[40] Masayuki Kubo, Junichiro Yamaguchi, Palladium-

catalyzed transfer nitration using β-nitrostyrenes as organic nitro reagents, *Chemistry Letters*, **2026**,55,(2), ,upag023, https://doi.org/10.1093/chemle/upag023.
[41] An, Da-Lie; et al, Bio-Inspired Consecutive Photocatalyzed C-H Nitration of Arenes, *Journal of Organic Chemistry* **2025**, 90(12), 4313-4324. https://doi.org/10.1021/acs.joc.5c00024.
[42] Qilin Xu, Jingli Dai, Fucheng Zhu, Yongjun Zang, Guosi Li, Chaoyue Sun, Fengxia An, Dong Liu, Yidong Zhong, Maoliang Liao; Two-Step Continuous Synthesis of Cabozantinib in a Microreactor: Mechanism and Kinetics Research of EDCI/HOBt-Mediated Amidation. *Ind. Eng. Chem. Res.* **2025**; 64 (1): 322–333. https://doi.org/10.1021/acs.iecr.4c04100.
[43] DWIVEDI, A. K. A. N. K. S. H. A. (no date) "Mechanism of Action, Synthesis, Properties and Analytical Methods of Cabozantinib," *International Journal of Applied Pharmaceutics*, **2023**,10.22159/IJAP.2023V15I1.46409.
[44] Shakeel, F.; Haq, N.; Alshehri, S.; Alsarra, I.A. Solubility and Thermodynamics Data of Cabozantinib Malate in Various Aqueous Solutions of Dimethyl Sulfoxide at Different Temperatures. *Molecules* **2023**, *28*, 7805. https://doi.org/10.3390/molecules28237805.
[45] Xiaobin Liang, Xiaorong Zhou, Yian Luo, An Su, Hanqi Zhou, Jianli Chen, Fengfan Liu, Weike Su; Four-Step Continuous-Flow Total Synthesis of 4-Chloro-6,7-dimethoxyquinoline, a Key Intermediate for Tyrosine Kinase Inhibitors. *Org. Process Res. Dev.* 17 July 2026; 30 (7): 2054–2066. https://doi.org/10.1021/acs.oprd.6c00170
[46] Anandhavalli Jeevarathinam, Sundaravadivel Elumalai; Mechanochemical Solvent-Free Introduction of Oxygen-Deficient in $NiCoMoO_4$ for High-Performance Energy Storage Applications. *Energy Fuels* , **2025**; 39 (47): 22605–22621. https://doi.org/10.1021/acs.energyfuels.5c04302.
[47] Suginome, S., Murota, K., Yamamoto, A. *et al.* Mechanochemical nitrogen fixation catalysed by molybdenum complexes. *Nat. Synth* , **2025**, 4,243–251,https://doi.org/10.1038/s44160-024-00661-y.
[48] J. M. Marrett, F. Effaty, X. Ottenwaelder, and T. Friščić, " Mechanochemistry for Metal–Organic Frameworks and Covalent–Organic Frameworks (MOFs, COFs): Methods, Materials, and Mechanisms." *Adv. Mater.* **2025**,37, (52): 2418707. https://doi.org/10.1002/adma.202418707.
[49] Głowniak, S.; Szczęśniak, B.; Choma, J.; Jaroniec, M. Mechanochemical Synthesis of MOF-303 and Its CO_2 Adsorption at Ambient Conditions. *Molecules* **2024**, *29*, 2698. https://doi.org/10.3390/molecules29112698.
[50] Amrute AP, De Bellis J, Felderhoff M, Schüth F. *Mechanochemical Synthesis of Catalytic Materials Chemistry*. **2021**, **27**(23):6819-6847. 10.1002/chem.202004583.
[51] Sajith, Ayyiliath M.; Muralidharan, Arayambath; Karuvalam, Ranjith P.; Haridas, Karickal R., Cross-coupling reaction of 2-halo-1-methyl-1H-imidazo[4,5-b]pyridine offers a new synthetic route to mutagenic heterocyclic amine-PHIP and DMIP, Journal of the *Korean Chemical Society* **2013**, 57(3), 361-364, 10.5012/jkcs.2013.57.3.361
[52] Liu, Kunjal Patel,; Anand Patel,; Vibhutiba P. Jethwa,; Hetal Patel, X-ray diffraction analysis of orthorhombic SnSe nanoparticles by Williamson–Hall, Halder–Wagner and Size–Strain plot methods, *Chemical Physics Impact*, **2024** (8), 100547, https://doi.org/10.1016/j.chphi.2024.100547.
[53] Fu, X.; Liu, Y.; Liu, Q.; Liu, Z.; Peng, Z. Preparation of Highly Active Cu/SiO_2 Catalysts for Furfural to 2-Methylfuran by Ammonia Evaporation Method. *Catalysts* **2022**, *12*, 276. 10.3390/catal12030276.
[54] Hexuan Zhang, Qi Zeng, Song Song, Wuyu Zhao, Xingang Li, Synergistic effect of Cu and Mo over Cu–Mo–SiO2 catalyst prepared by sol-gel method for high-efficient and stable de-methoxylation of lignin-derived 4-propylguaiacol,*Molecular Catalysis*, **2025,** 570,114697, https://doi.org/10.1016/j.mcat.2024.114697.
[55] Xinhui Li, Ruiheng Zhu, Baoquan Sun, Like Chen, Hongwei Yang, Xiaohui Liu, Yong Guo, Yanqin Wang, Cu@SiO2 catalyst with high copper dispersion for chemoselective hydrogenation of p-chloronitrobenzene,*Chemical Engineering Journal*, 487**,2024**,150652, https://doi.org/10.1016/j.cej.2024.150652.
[56] Sohrab Nasiri, Marzieh Rabiei, Arvydas Palevicius, Giedrius Janusas, Andrius Vilkauskas, Venkatramaiah Nutalapati, Ahmad Monshi,Modified Scherrer equation to calculate crystal size by XRD with high accuracy, examples Fe2O3, TiO2 and V2O5,*Nano Trends*,**2023**, 3,100015, https://doi.org/10.1016/j.nwnano.2023.100015.
[57] Gulyaeva, Y.; Alekseeva, M.; Bulavchenko, O.; Kremneva, A.; Saraev, A.; Gerasimov, E.; Selishcheva, S.; Kaichev, V.; Yakovlev, V. Ni–Cu High-Loaded Sol–Gel Catalysts for Dehydrogenation of Liquid Organic Hydrides: Insights into Structural Features and Relationship with Catalytic Activity. *Nanomaterials* **2021**, *11*, 2017. https://doi.org/10.3390/nano11082017.
[58]Patterson,; Paulina Summa,;Katarzyna Świrk Da Costa,; Li Li,Monika Motak ,;Marta Gajewska,;Changwei Hu,; Patrick Da Costa,; *Applied Catalysis B: Environment and Energy* **2026**,(*382*) 125986, https://doi.org/10.1016/j.apcatb.2025.125986
[59] Penny Mathumba,;Mawethu P Bilibana,;Olalekan C Olatunde,; Damian C Onwudiwe,Saddle, X-ray diffraction profile analysis of green synthesized ZnO and TiO2 *nanoparticles, Materials Research Express*, **2024** ,(11),7 10.1088/2053-1591/ad63ff.
[60] Mahtab Vosough, Gholam Reza Khayati, Shahriar Sharafi,Thermal kinetics study on the conversion of β-MoO3 to α-MoO3; A molybdenite concentrate

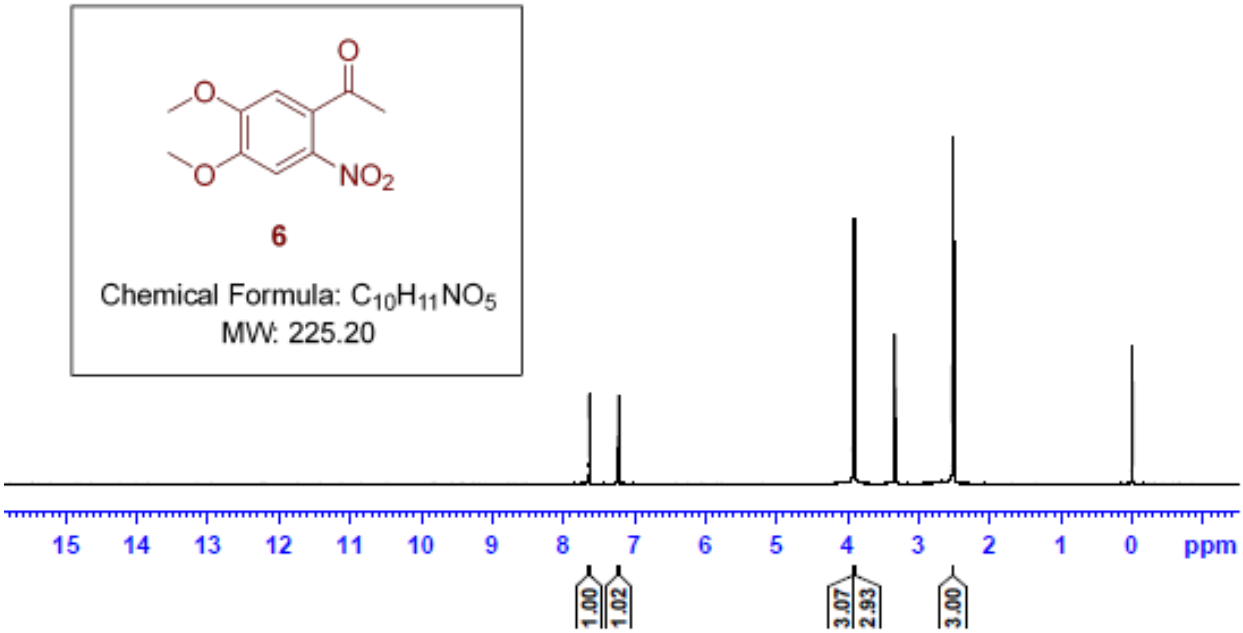
derivative as a catalyst, *Thermochimica Acta,* **2022,**715, 179289, https://doi.org/10.1016/j.tca.2022.179289.
[61] Fan, W.W., Gualtieri, A.F., Hamilton, A. *et al.* Determining factors affecting the accuracy of SEM-EDX data-based quantitative chemical analysis for identifying naturally occurring individual carcinogenic erionite fibres. *Sci Rep* ,**2025**,15, 25316 (). https://doi.org/10.1038/s41598-025-09551-5.
[62] Paul C. Guyett, David Chew, Vitor Azevedo, Lucy C. Blennerhassett, Carolina Rosca, Emma Tomlinson; Optimizing SEM-EDX for fast, high-quality and non-destructive elemental analysis of glass. *J. Anal. At. Spectrom.* **2024**; 39 (10): 2565–2579. https://doi.org/10.1039/d4ja00212a.
[63] Sammad A, Iqbal J, Ahmad N, Hedwig R, Asghar H, Umar ZA, Baig MA, Ahmed R. Elemental analysis of molybdenum ore using charge coupled device (CCD) and intensified charge-coupled device (ICCD) based LIBS systems. *Rev Sci Instrum.* **2025**;96(9):093003. 10.1063/5.0277624.
[64] Nadeem Baig, Irshad Kammakakam, Wail Falath; Nanomaterials: a review of synthesis methods, properties, recent progress, and challenges. *Mater. Adv.* **2021**; 2 (6): 1821–1871. https://doi.org/10.1039/d0ma00807a.
[65] Sadeghi, S., Maleki, B. A recyclable dendrimeric Ni nanocatalyst anchored on magnetic nanoparticles for the green reduction of nitroarene pollutants and one-pot synthesis of imines. *Sci Rep* **(2026)**,16, 6594 https://doi.org/10.1038/s41598-026-35919-2
[66] Lungu,;T. Potlog.; M. Dobromir,; and S. Moldovan, Investigating the Impact of the Calcination Temperature on the Structural Properties and Composition of $NaMgF_3$,NPS.,*ChemistrySelect* ,**2026,** 11, (3) e05915.,https://doi.org/10.1002/slct.202505915
[67] Saeedi Z, Sorouraddin SM, Farajzadeh MA, Afshar Mogaddam MR, Bakhshi A. Dispersive solid phase extraction using SiO_2@ZIF-8@Fe_3O_4 core-shell nanoparticles for extraction of Cd(ii), Zn(ii), and Cu(ii) ions from fruit juice samples. *RSC Adv*. **2025**, Dec 8;15(56):47913-47924. 10.1039/d5ra06835e.
[68] Qu J, Sui M, Li R. Recent advances in *in-situ* transmission electron microscopy techniques for heterogeneous catalysis. *iScience*. **2023** ;26(7):107072.,10.1016/j.isci.2023.107072.
[69] Idan Biran, Lothar Houben, Anna Kossoy, Boris Rybtchinski; Transmission Electron Microscopy Methodology to Analyze Polymer Structure with Submolecular Resolution. *J. Phys. Chem. C*., **2024**; 128 (14): 5988–5995. https://doi.org/10.1021/acs.jpcc.3c06977.
[70] Zhong, X.; Liang, G.; Meng, L.; Xi, W.; Gu, L.; Tian, N.; Zhai, Y.; He, Y.; Huang, Y.; Jin, F.; et al. Automated Particle Size Analysis of Supported Nanoparticle TEM Images Using aPre-TrainedSAMModel. *Nanomaterials* **2025**, *15*,1886. https://doi.org/10.3390/nano15241886.
[71] Kristen M. Aviles, Benjamin J. Lear; Practical Guide to Automated TEM Image Analysis for Increased Accuracy and Precision in the Measurement of Particle Size and Morphology. *ACSNanosci,***2025**;5,(3):117-127, https://doi.org/10.1021/acsnanoscienceau.4c00076.
[72] Zhang S, Wang C. Precise Analysis of Nanoparticle Size Distribution in TEM Image. *Methods Protoc*, **2023**;6(4):63. 10.3390/mps6040063.
[73] Sergey K. Filippov, Ramil Khusnutdinov, Anastasiia Murmiliuk, Wali Inam, Lucia Ya. Zakharova, Hongbo Zhang, Vitaliy V. Khutoryanskiy; Dynamic light scattering and transmission electron microscopy in drug delivery: a roadmap for correct characterization of nanoparticles and interpretation of results. Mater. Horiz. 2023;10,(12):5354–5370. https://doi.org/10.1039/d3mh00717k.
[74] M. Ek, S. Cheong, J. Cairney, R. D. Tilley, and I. Persson, " Using In Situ TEM to Understand the Surfaces of Electrocatalysts at Reaction Conditions: Single-Atoms to Nanoparticles." *Adv. Funct. Mater***,2026**. 36, ,11 , e14614. https://doi.org/10.1002/adfm.202514614.
[75] Lazar Bijelić, Francisco Ruiz-Zepeda, Nejc Hodnik; The role of high-resolution transmission electron microscopy and aberration corrected scanning transmission electron microscopy in unraveling the structure–property relationships of Pt-based fuel cells electrocatalysts. *Inorg. Chem. Front.* **2024**; 11 (2): 323–341. https://doi.org/10.1039/d3qi01998e.
[76] Liu, J.; Yang, J.; Zhang, C. Positioning of Nanoscale Materials in TEM: A Method Based on Image Comparison in a Specific Micro-Domain. *Appl. Sci.* **2025**, *15*, 12026. https://doi.org/10.3390/app152212026.

Content:

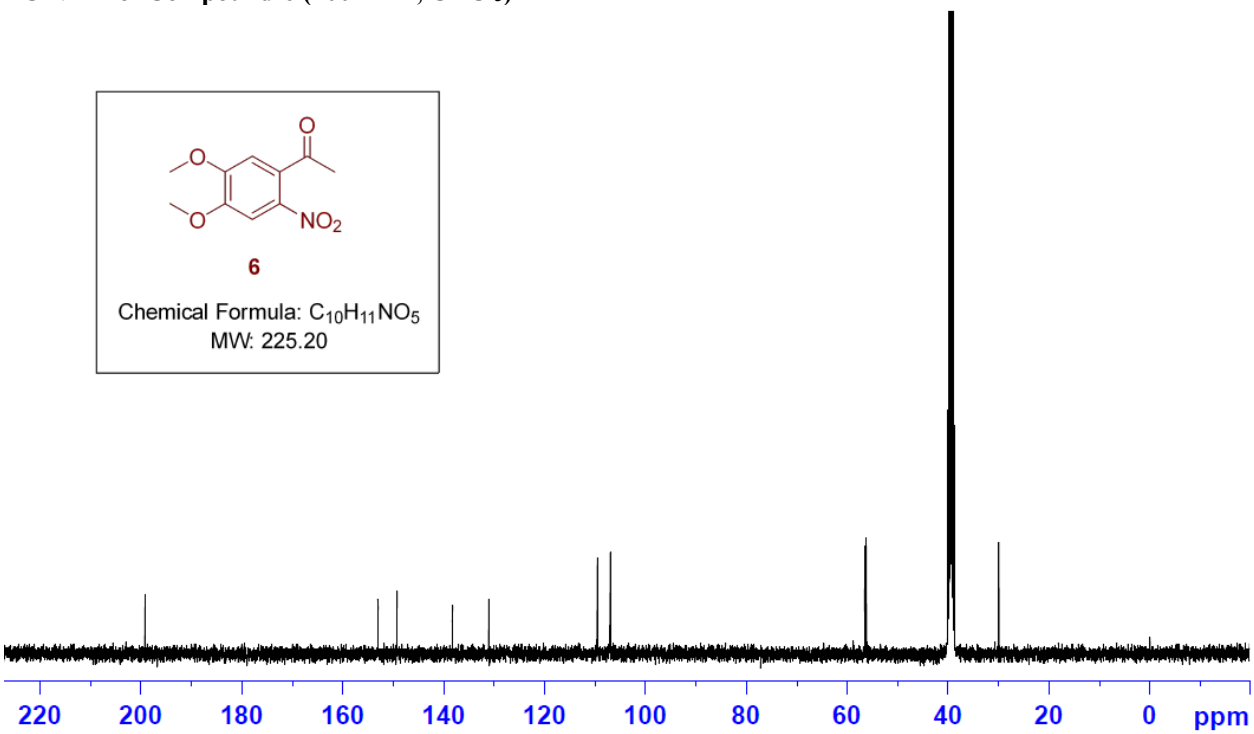
1. 1H NMR of **Compound-6** Page-S1
2. 13C NMR of **Compound-6** Page-S1
3. 1H NMR of **Compound-7** Page-S2
4. 13C NMR of **Compound-7** Page-S2
5. 1H NMR of **Compound-8** Page-S3
6. 13C NMR of **Compound-8** Page-S3
7. 1H NMR of **Compound-9** Page-S4
8. 13C NMR of **Compoun-9** Page-S4
9. 1H NMR of **Compound-10** Page-S5
10. 13 C NMR of **Compound-10** Page-S5

11. 1H NMR of **Compound-11** Page-S6
12. 13C NMR of **Compound-11** Page-S6
13. 1H NMR of **Compound-12** Page-S7
14. 13C NMR of **Compound-12** Page-S7
15. 1H NMR of **Compound-13** **Page-S8**
16. 13C NMR of Compound-13 **Page-S8**

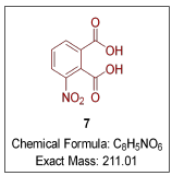
^{1}H NMR of Compound-6 (400 MHz, $CDCl_3$)

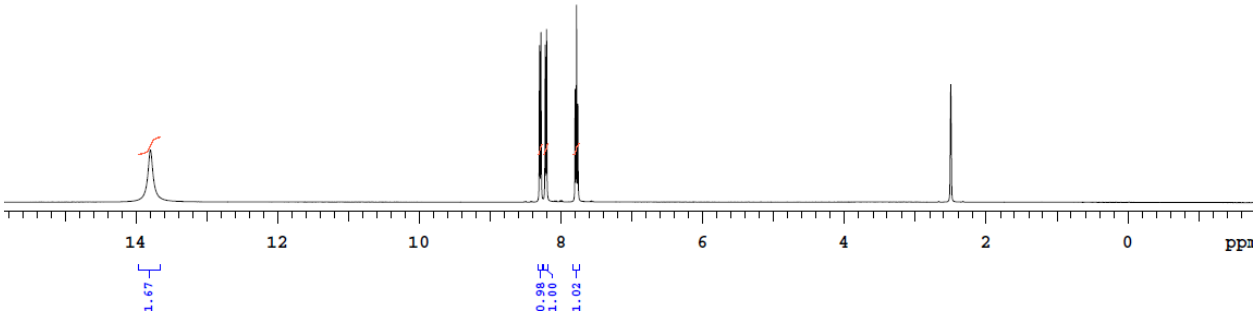


^{13}C NMR of Compound-6 (400 MHz, $CDCl_3$)

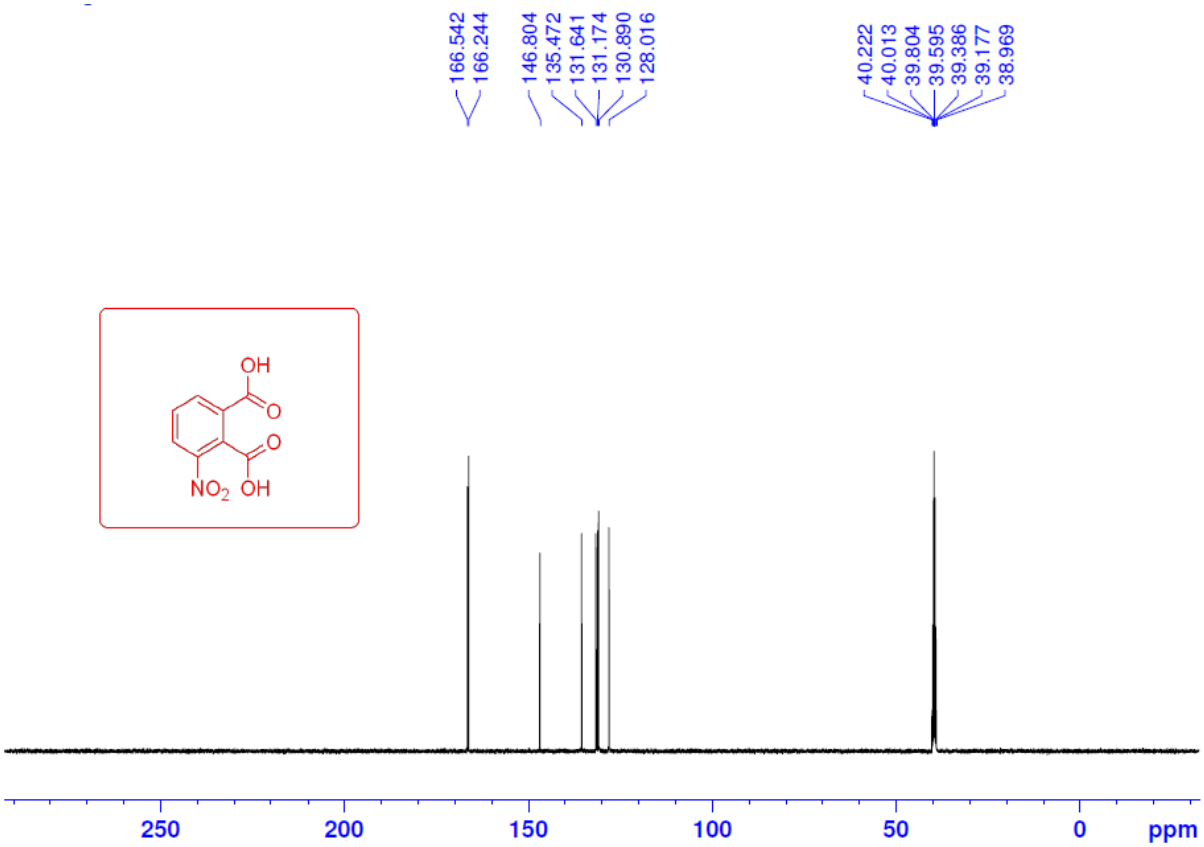


^{1}H NMR of Compound-7 (400 MHz, $CDCl_3$)

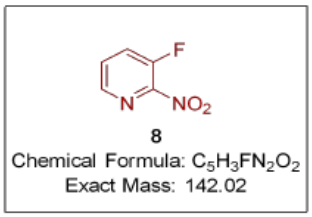


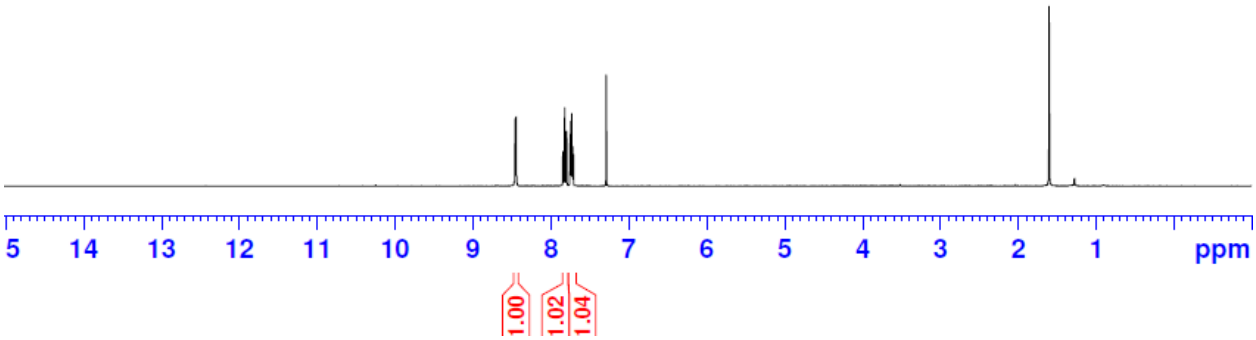


^{13}C NMR of Compound-7 (400 MHz, $CDCl_3$)

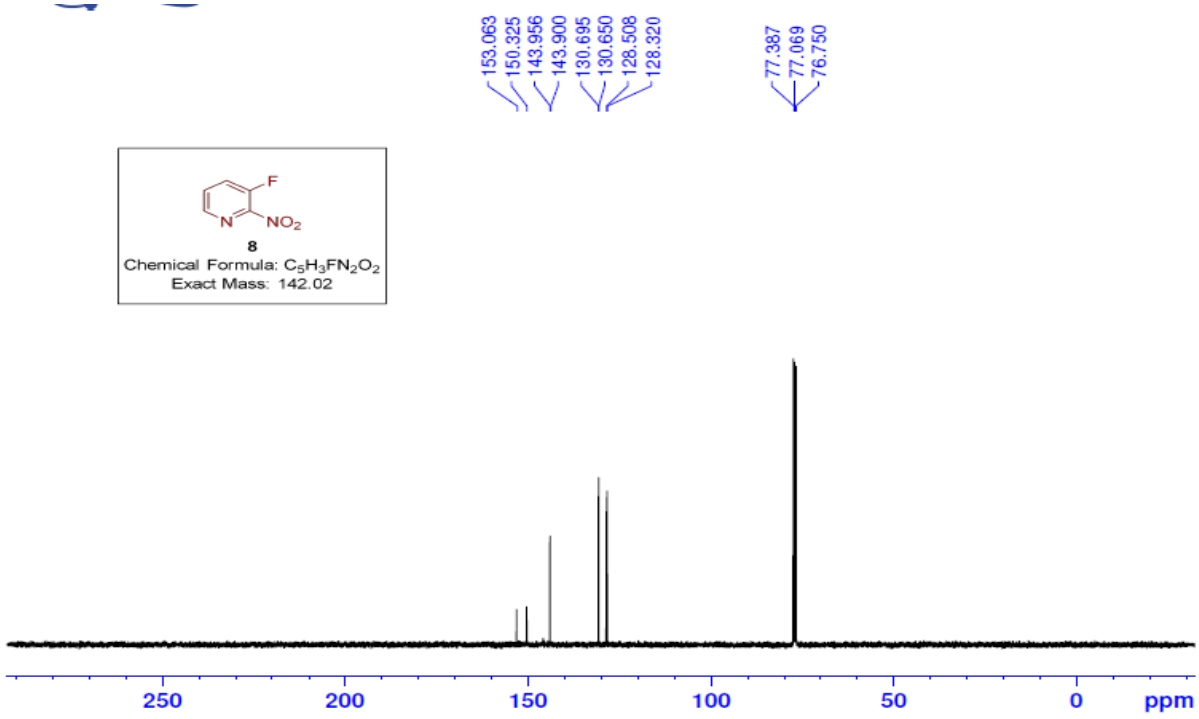


^{1}H NMR of Compound-8 (400 MHz, $CDCl_3$)

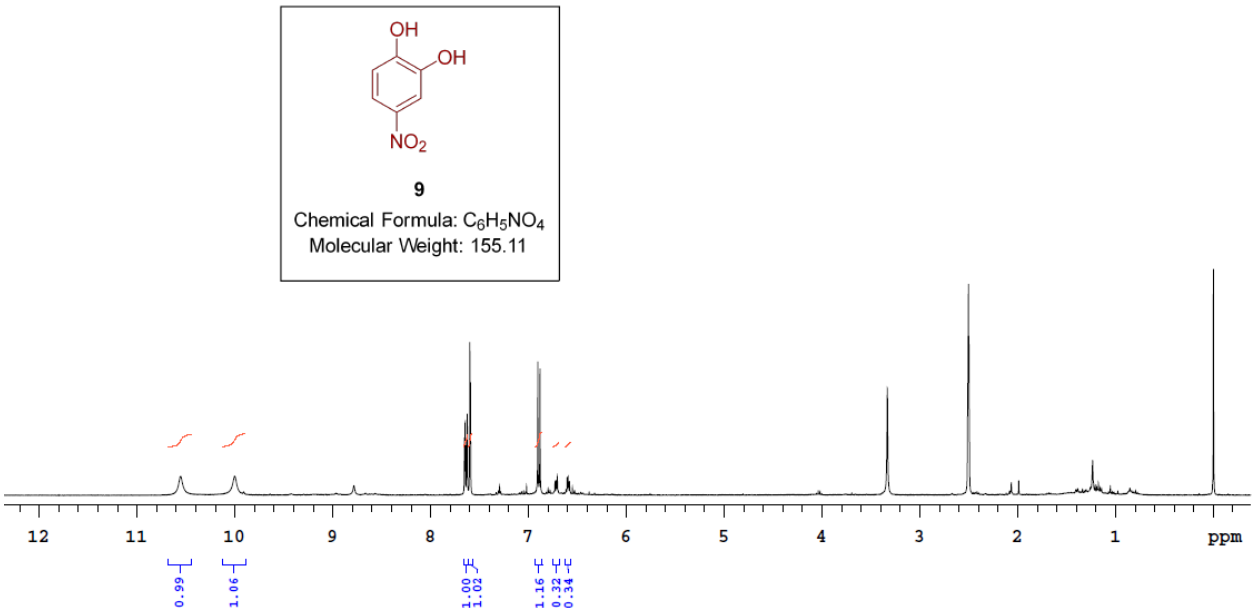




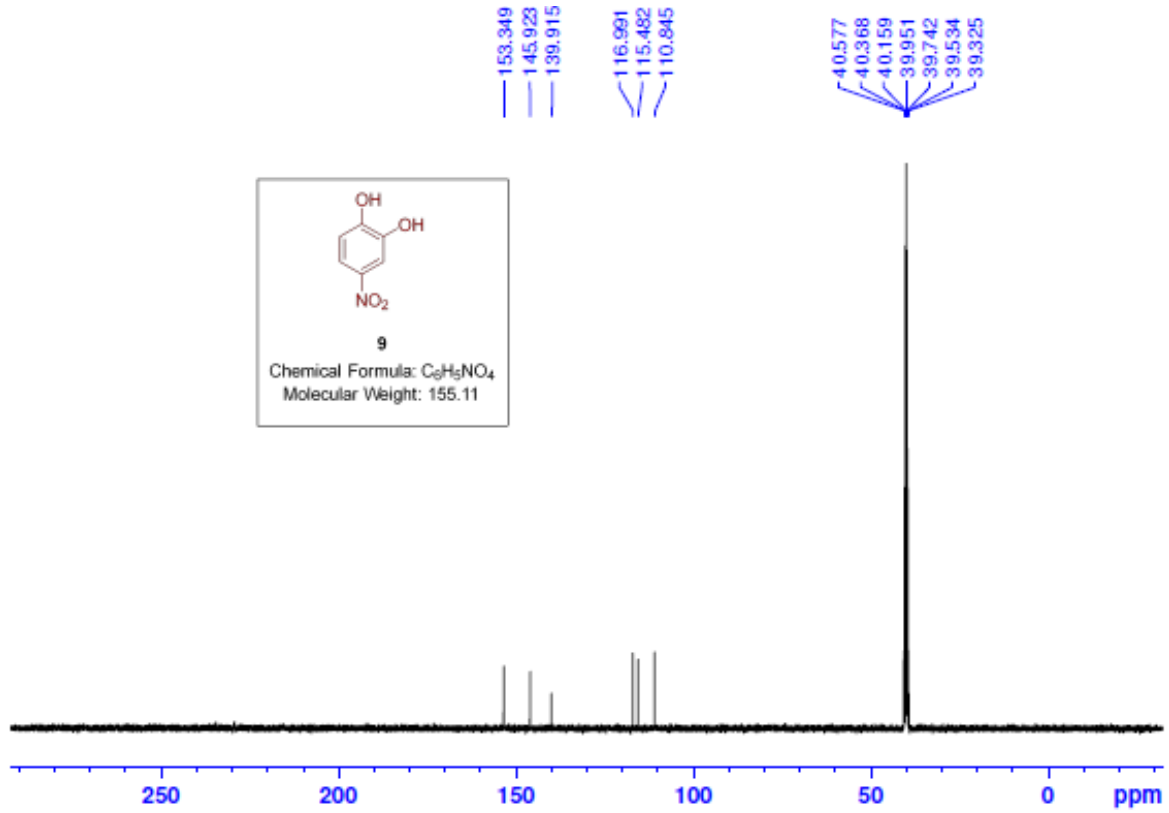
^{13}C NMR of Compound-8 (400 MHz, $CDCl_3$)



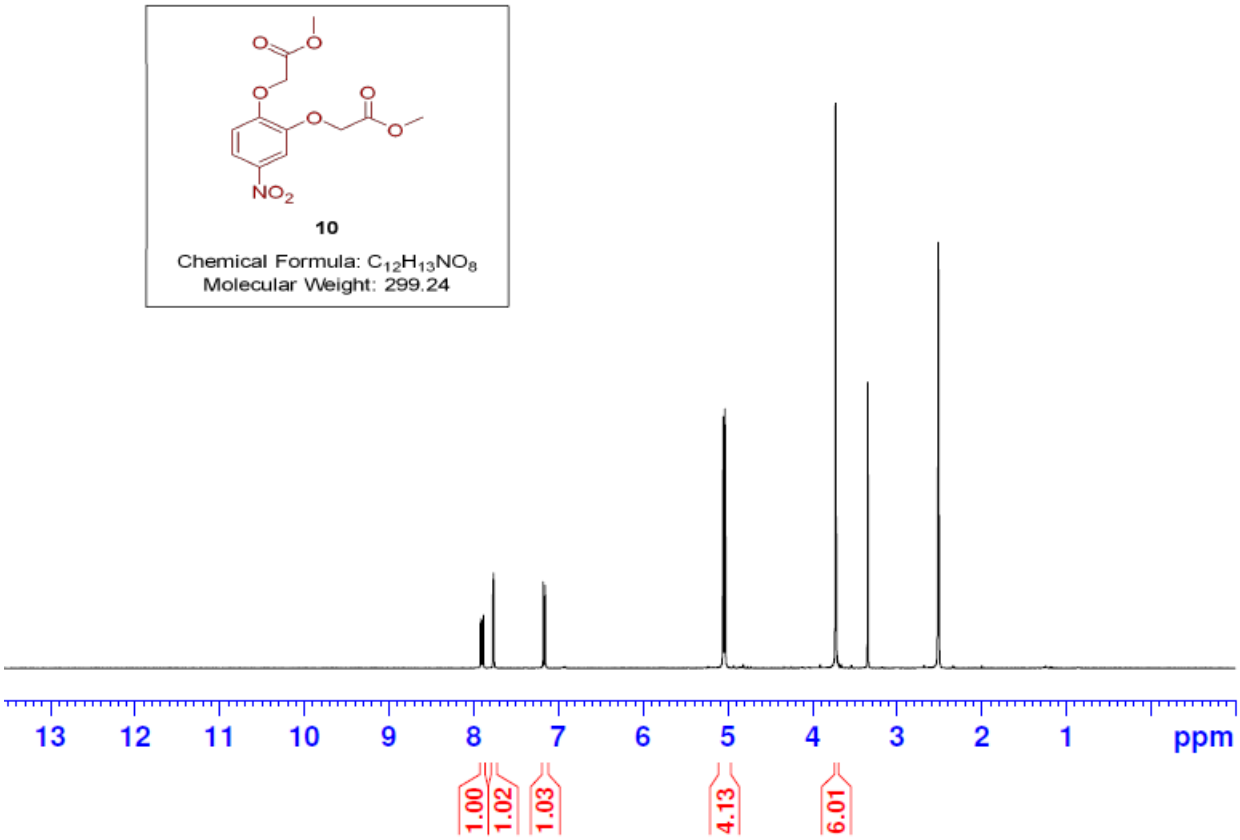
^{1}H NMR of Compound-9 (400 MHz, $CDCl_3$)



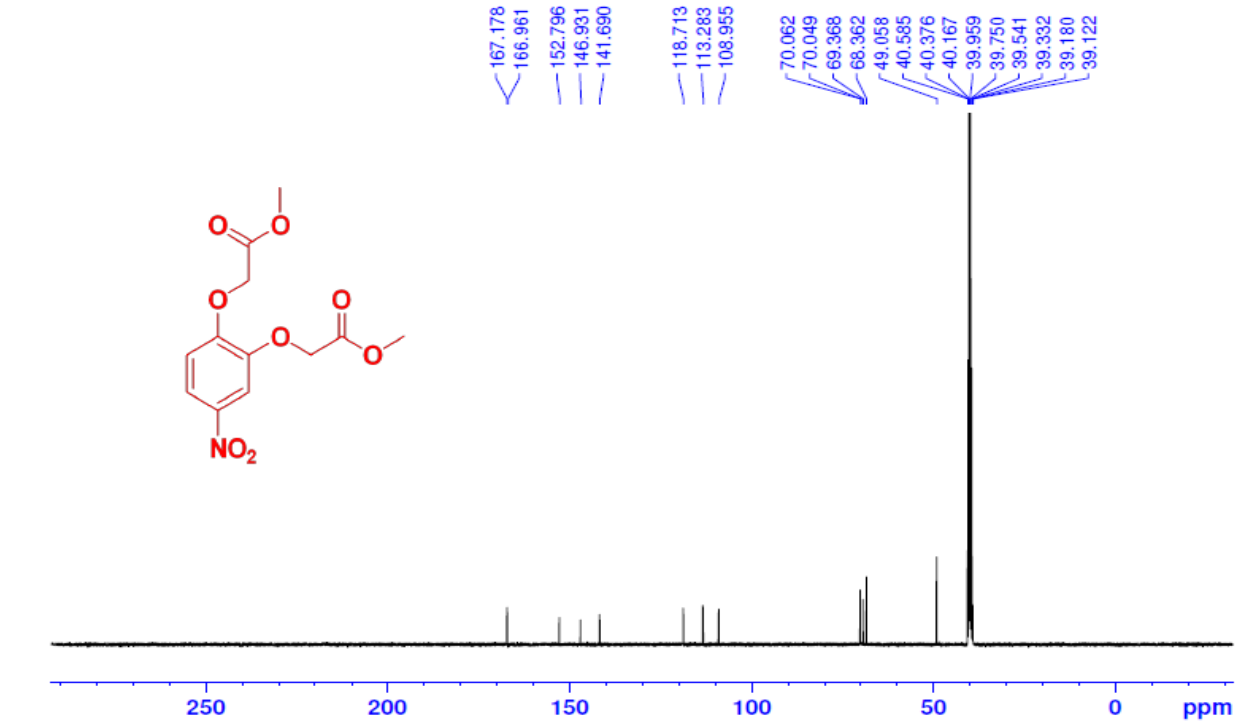
^{13}C NMR of Compound-9 (400 MHz, $CDCl_3$)



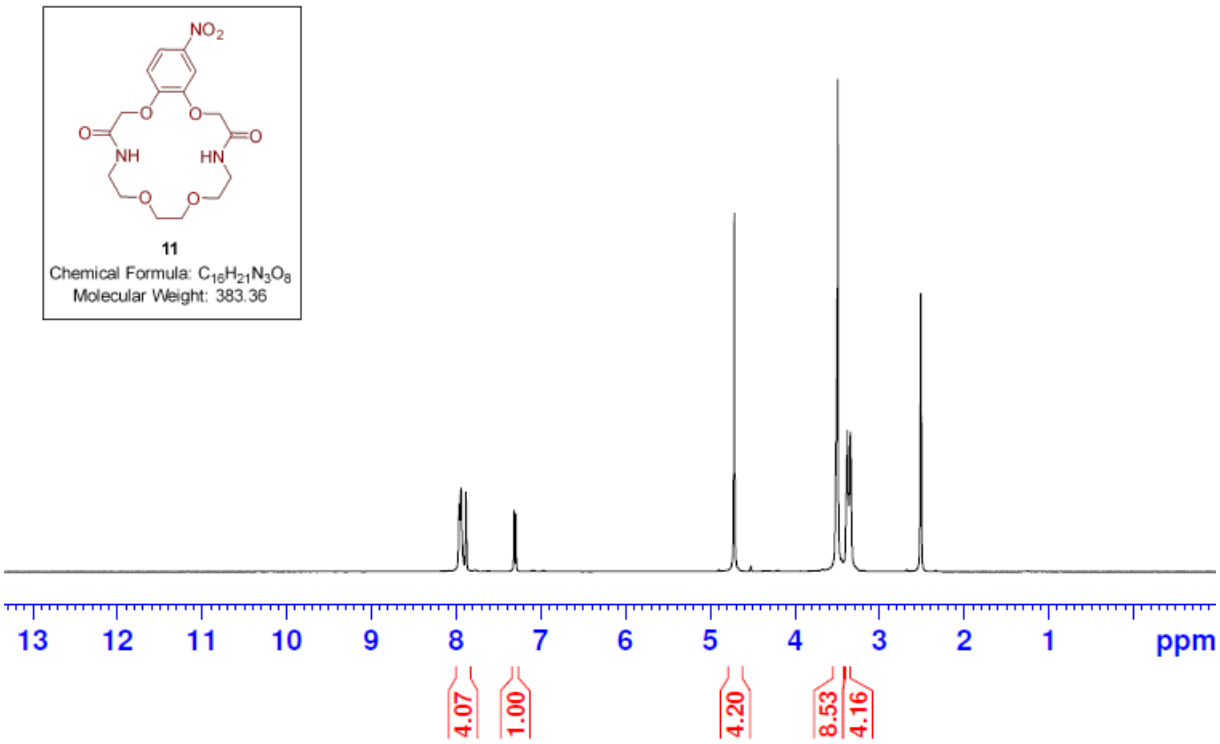
^{1}H NMR of Compound-10 (400 MHz, $CDCl_3$)



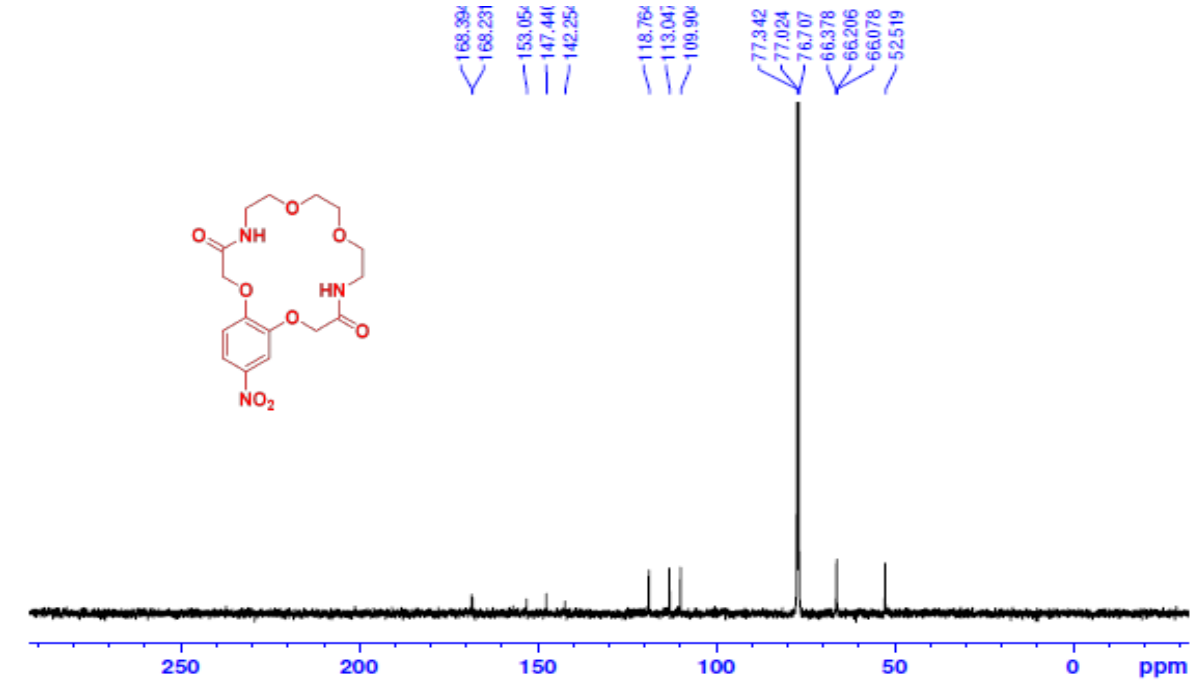
^{13}C NMR of Compound-10 (400 MHz, $CDCl_3$)



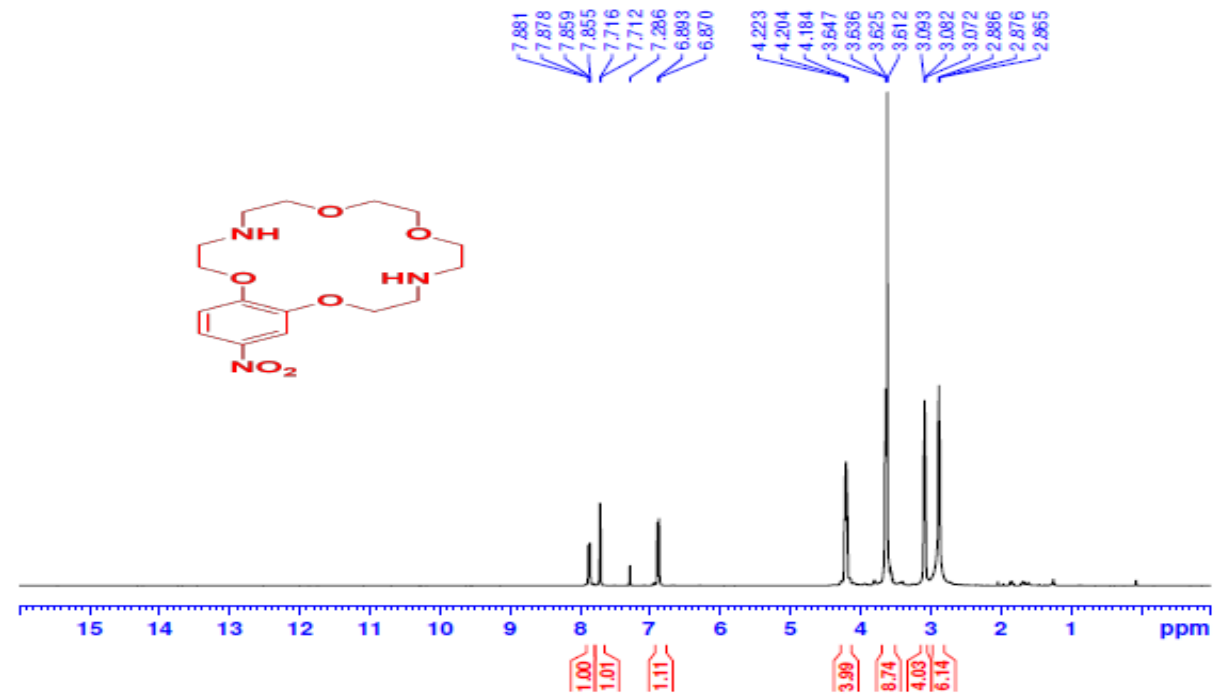
^{1}H NMR of Compound-11 (400 MHz, $CDCl_3$)



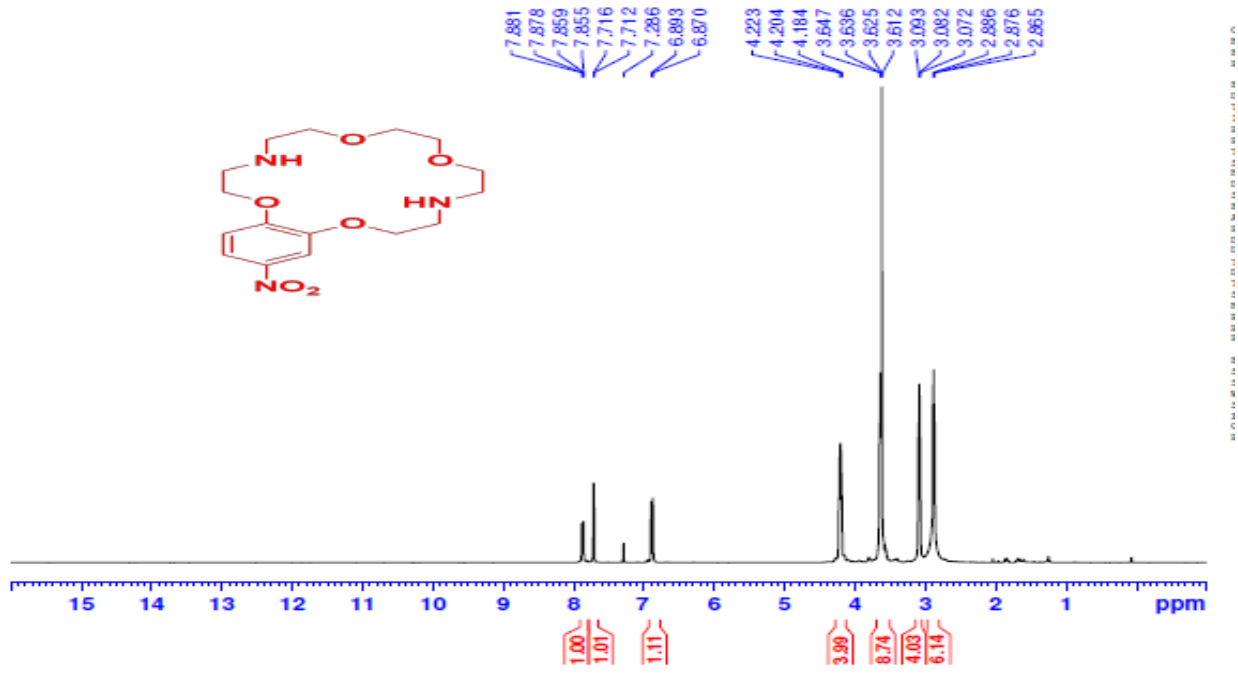
^{13}C NMR of Compound-11 (400 MHz, $CDCl_3$)



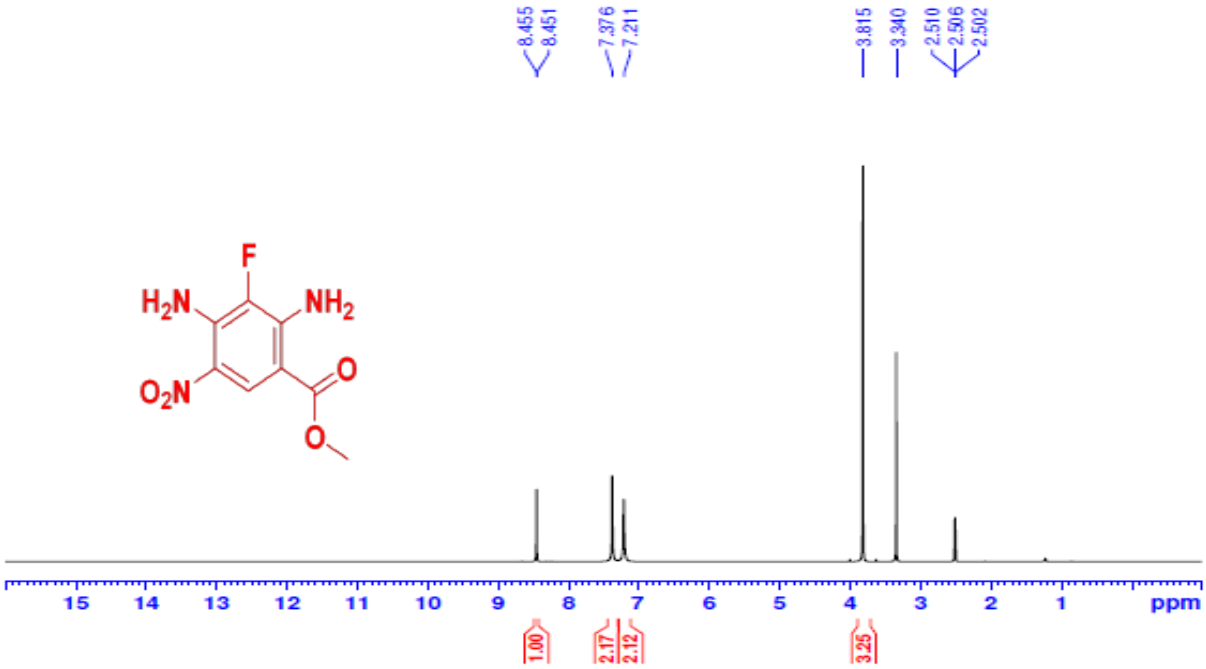
^{1}H NMR of Compound-12 (400 MHz, $CDCl_3$)



^{13}C NMR of Compound-12 (400 MHz, $CDCl_3$)



^{1}H NMR of Compound-13 (400 MHz, $CDCl_3$)



^{13}C NMR of Compound-13 (400 MHz, $CDCl_3$)

